

AD-A011 110

VERTICAL DIRECTIONALITY OF NOISE AND
SIGNAL TRANSMISSIONS DURING OPERATION
CHURCH ANCHOR

Victor C. Anderson

Scripps Institution of Oceanography
San Diego, California

15 November 1974

DISTRIBUTED BY:



National Technical Information Service
U. S. DEPARTMENT OF COMMERCE

Best Available Copy

ADAO11110

178064



MARINE PHYSICAL LABORATORY
of the Scripps Institution of Oceanography
San Diego, California 92132

VERTICAL DIRECTIONALITY OF NOISE AND SIGNAL
TRANSMISSIONS DURING OPERATION CHURCH ANCHOR

Victor C. Anderson

Sponsored by
Office of Naval Research
N00014-69-A-0200-6002
NR 260-103

Reproduction in whole or in part is permitted
for any purpose of the U.S. Government

Document cleared for public release
and sale; its distribution is unlimited

15 November 1974

SIO REFERENCE 75-1

Reproduced by
**NATIONAL TECHNICAL
INFORMATION SERVICE**
U.S. Department of Commerce
Springfield, VA 22151

Best Available Copy

UNCLASSIFIED

SECURITY CLASSIFICATION OF THIS PAGE (When Data Entered)

REPORT DOCUMENTATION PAGE		READ INSTRUCTIONS BEFORE COMPLETING FORM
1. REPORT NUMBER SIO Reference 75-1	2. GOVT ACCESSION NO.	3. RECIPIENT'S CATALOG NUMBER <i>AD-A01110</i>
4. TITLE (and Subtitle) VERTICAL DIRECTIONALITY OF NOISE AND SIGNAL TRANSMISSIONS DURING OPERATION CHURCH ANCHOR		5. TYPE OF REPORT & PERIOD COVERED Summary
7. AUTHOR(s) Anderson, Victor C.		6. PERFORMING ORG. REPORT NUMBER MPL-U-53/74
8. CONTRACT OR GRANT NUMBER(s) N00014-69-A-0200-6002		9. PROGRAM ELEMENT, PROJECT, TASK AREA & WORK UNIT NUMBERS 712408
11. CONTROLLING OFFICE NAME AND ADDRESS Office of Naval Research, Code 210, Department of the Navy, Arlington, Virginia 22217		12. REPORT DATE 15 November 1974
14. MONITORING AGENCY NAME & ADDRESS (if different from Controlling Office)		13. NUMBER OF PAGES <i>55</i>
16. DISTRIBUTION STATEMENT (of this Report)		15. SECURITY CLASS. (of this report) Unclassified
		15a. DECLASSIFICATION/DOWNGRADING SCHEDULE
17. DISTRIBUTION STATEMENT (of the abstract entered in Block 20, if different from Report)		
18. SUPPLEMENTARY NOTES		
19. KEY WORDS (Continue on reverse side if necessary and identify by block number) vertical directionality, processor, beamformer, ambient noise, background noise, propagation, directional spectra		
20. ABSTRACT (Continue on reverse side if necessary and identify by block number) A vertical array of 20 vibration isolated hydrophones was suspended from the Research Platform R/P at various depths from 713m to 4816m. Preformed sets of beams were formed with a digital beamformer to observe the vertical noise distribution at 3 to 4 frequencies between 20 and 100 Hz. Directional spectra derived from 10 minutes samples of digital records are presented. Several contour plots of amplitude distributions are also shown for both signal and noise records.		

DD FORM 1 JAN 73 EDITION OF 1 NOV 72
5400-100-014-6601

SOLENE

UNCLASSIFIED

SECURITY CLASSIFICATION OF THIS PAGE WHEN FIRST ENTERED

PRICES SUBJECT TO CHANGE

MARINE PHYSICAL LABORATORY
of the Scripps Institution of Oceanography
San Diego, California 92152

VERTICAL DIRECTIONALITY OF NOISE AND SIGNAL
TRANSMISSIONS DURING OPERATION CHURCH ANCHOR

Victor C. Anderson

Sponsored by
Office of Naval Research
N00014-69-A-0200-6002
NR 260-103

SIO REFERENCE 73-1

15 November 1971

Reproduction in whole or in part is permitted
for any purpose of the U.S. Government

Document cleared for public release
and safety; its distribution is unlimited

E. N. SPILLER, DIRECTOR

VERTICAL DIRECTIONALITY OF NOISE AND SIGNAL
TRANSMISSIONS DURING OPERATION CHURCH ANCHOR

Victor C. Anderson

University of California, San Diego
Marine Physical Laboratory of the
Scripps Institution of Oceanography
San Diego, California 92132

ABSTRACT

A vertical array of 20 vibration isolated hydrophones was suspended from the Research Platform FLIP at various depths from 713m to 4816m. Preformed sets of beams were formed with a digital beamformer to observe the vertical noise distribution at 3 to 4 frequencies between 20 and 100 Hz. Directional spectra derived from 10 minutes samples of digital records are presented. Several contour plots of amplitude distributions are also shown for both signal and noise records.

INTRODUCTION

During the first part of operation CHURCH ANCHOR, 20 hydrophones were configured in a uniformly spaced vertical linear array and lowered to various depths from FLIP. Part of the on board processing equipment for this array consisted of the TRAPP beamformer - a programmable narrow-band multibeam 8-bit digital beamformer which allowed observations to be made for a full set of uniformly spaced vertical beams at four frequencies of interest. The processor acted as a narrow-band filter at each of these frequencies thus, the observations should be considered to be estimates of the power spectrum level of the directional spectrum of the background noise in the ocean.

During the periods of time designated as "noise days" observations were made at sequential depth for a set of six predetermined depths. At each depth an observation time of 20 minutes was used during which time continuous recordings of the complete set of beams was made. The on-line monitor during recording was a Ross Recorder, an intensity type recorder generating four parallel time bearing plots one plot for each of the four frequencies. The detected beam outputs which represent the intensity on these plots were formatted in a serial scan which was recorded on digital tape for later processing.

During the propagation runs data were also collected with this system. In this case, recordings were made during transmission periods but the depth of the array was controlled by the requirements of the propagation runs rather than by the vertical directionality experiments. The propagation array data analyzed to date only indicate the gross directional structure, however, the frequency sets were chosen so that one nearby frequency was recorded at the same time as a signal frequency so that some indication of the background noise level through the gain of the array could be obtained.

The data sets of this report are grouped by experiment. For each experiment the data are presented by way of graphs which represent the vertical noise distribution at the four frequencies involved. The graphs are of two types; one is a plot of mean power values computed from accumulated histograms of 10-minute samples of the beam output scans, the other, a contour plot which is derived from the same data but represents the contours of the histograms of the beamformer output samples. A considerable amount of post processing has been applied to the data for the purpose of smoothing the histograms and removing some of the anomalies of the equipment which were discovered in the data analysis.

An extensive effort was spent in looking at the process of deconvolution of the beamformer outputs with the goal of improving the estimate of the directional noise field. This work has been reported in the literature.^{1,2} The results of this effort show that the deconvolution process for this particular uniformly spaced linear array is of marginal benefit. Because the process is very sensitive to the fine structure of the theoretical beam pattern, it was felt that there may be enough uncertainties in the linearity of the array or in the linearity of the wavefront arrivals that the application of the deconvolution algorithm might actually degrade the estimate of the directional distribution. Therefore, only the unmodified beam output power of the array has been presented here. There are two artifacts of the instrumentation which occur and are particularly prominent in the case of the background noise recordings.

First, there is a significant amount of what is interpreted as common mode noise which shows up as an output on the perpendicular beam which is the horizontal (90°) beam. The question of whether or not this common mode noise could be subtracted out of the directional patterns in a valid way was considered carefully; there was insufficient consistency from record to record in the level of this common mode noise to justify any subtraction so no attempt has been made to take it out of the data presented here.

Second, the narrow band filter had extended sidelobe responses which lay, on the average, 40 dB below the response in the pass band. Thus noise power uniformly distributed over a 300 Hz band will give rise to a filter output power which is only a few dB below the inband noise power. This effect places a floor on the minimum noise bands which can be measured for the background noise records but does not seriously affect the signal transmission runs where the major energy was concentrated in a few frequencies.

INSTRUMENTATION

The array which was used consisted of 20 of the hydrophones using the Whitney suspension cage design shown in Fig. 1. The elements are independently suspended in a very low compliance elastic suspension within the external support cage. The hydrophones outputs are amplified and coupled through an FM telemetry link over the single coaxial cable to FTFP where a set of 20 receivers demultiplex and demodulate the signals for processing by the beamformer. The characteristics of the beamformer are summarized in Table 1.² The 20 hydrophones of the array are interconnected to form a uniformly spaced array with an overall length of 332 meters and an effective length of 360 meters. Figure 2 shows the six array depths used during the noise measurement periods.



Fig. 1. Whitney hydrophone cage assembly.

The set of frequencies used with the array range from 33 Hz to 200 Hz and thus a wide variation in beam patterns will be observed. A characteristic set of patterns are given in Figs. 3 through 6. The patterns are presented here as a set of 131-1.3 samples corresponding to the beam centers. At 100 and 200 Hz, the pattern is undersampled and the peculiar side lobes are a consequence of nearly commensurate sampling period and main-pattern lobe widths. Above 30 Hz, grating lobes having amplitude responses as high as the main lobe of the array will be observed within the ±180° vertical angle set. At 200 Hz three sets of these grating lobes are to be observed.

The beamformer was programmed to generate four sets of beams for four selectable narrow-band frequencies. Each set covered the range of 0-180° with a 1-1/2° beam-to-beam spacing for a full set of 131 beams. The extreme beams were pointed vertically up (0°) and vertically down (180°). A single narrow band filter channel was synthesized in the beamformer by multiplying the time-multiplexed high speed audio beam data block by a 4-bit quantized sine and cosine reference signal at the center band frequency which had been amplitude weighted over the 1-second integration block to control the filter sidelobes. A finite time integrator operating over the 1-second data block provided the low-pass filter for the two cross-products

Table 1. Beamformer Specifications

ELECTRICAL CHARACTERISTICS

Inputs

- a. Number of channels: 1 to 48 (2 ea., DD50S conn).
- b. Impedance, single ended: 1 megohm.
- c. Impedance, transformer: 600 ohms.
- d. Maximum voltage: 3 volts (rms).
- e. Frequency band: 10 to 250 Hz, 500 Hz, 1000 Hz.
- f. Gain: 0 to + 75 dB in 5-dB increments.

Outputs

- a. Detected beam scans.
 - (1) Four quadrature element sums (1 to 12), 4-msec beams, 12-bit words, TTL compatible (4 ea., DAI5S).
 - (2) One, full-element sum (1 to 48), 4-msec beams, analog, low-impedance (coaxial) (also displayed on time-bearing recorder).
- b. Undetected beam outputs.
 - (1) One, full-element sum (1 to 18), 1024, 4-msec samples/beam, 12 bit-words, TTL compatible (1 ea., DAI5S) also internally formatted for writing every sixteenth beam onto magnetic tape.
 - (2) Same as (1) for EPI, but interfacing is yet to be determined.
- c. 4-msec and 4-msec clocks, TTL compatible (coaxial).

PHYSICAL CHARACTERISTICS

- a. Input power: 115 vac, 60 Hz, 40 amperes.
- b. Size: 1, 3-track bay = 6¹/3" x 5¹/3" x 2¹/4" plus wheels.
1, 1-track bay = 6¹/3" x 2¹/3" x 2¹/4" plus wheels.
- c. Weight: 1-track bay, 200 pounds,
3-track bay, 300 pounds.

terms. After low-pass filtering, the two cross-product terms were squared and then summed to produce the output power signal. The frequency response of this filter is shown in Fig. 7. As can be seen, it has an effective bandwidth of 0.5 Hz. It also reflects the effect of the 4-bit quantization of the reference signal in the extended side lobe levels which are only down about 10 dB. The gain corrections arising from the various portions of the system which must be applied to the data are summarized in Fig. 8.

PHASE I ARRAY POSITIONS RELATIVE TO THE VELOCITY PROFILE

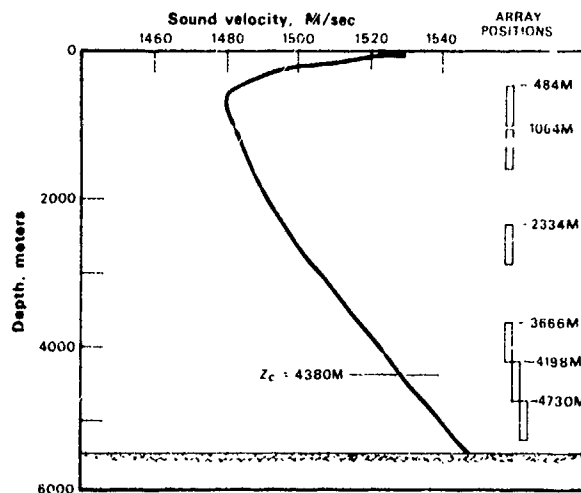


Fig. 2. Array positions relative to the velocity profile.

The beamformer records were analyzed in 10-minute blocks. Only the first 10-minute sample of each tape has been included in this report. For each 10-minute period, 300 2-second samples were combined to provide the average values. The distributions which were run on these samples are histograms for the 300-sample sets. A summary of the data sets is given in Table II. Summaries of the gain factors for the data sets are given in Table III. A high density of ship traffic occurred during the "noise days". Figures 9 and 10 show the time relationship of the depth station, ship traffic and data tapes.

DATA PROCESSING

Before proceeding to the directional plots a word of explanation of the data processing is in order. The format of the narrow-band beamformer data is a 9-bit floating point number representing the narrow-band energy in a 2-second sample. The number consists of a 5-bit exponent of base four and a 4-bit mantissa. The dynamic range is approximately 88 dB. The data are stored in 512 word records by a 9-track 800 bpi tape recorder. One tape record contains 2-second samples of 128 beams for four frequencies.

The chronological sequence for the data processing was as follows: the tapes were read by the Burroughs 6700 computer at 1000D using a routine which converted the base four floating point numbers to Burroughs 18-bit words. Three hundred records representing 10 minutes of real time data were inverted and sorted by Beam number and Frequency at one pass. The sorted data were then grouped into 12 dB wide

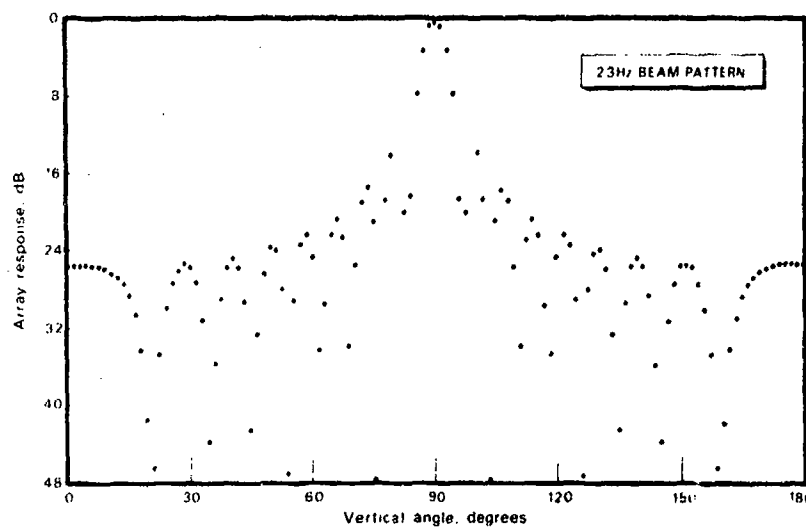


Fig. 3. Theoretical response of the beamformer to a horizontal plane wave at 23 Hz.

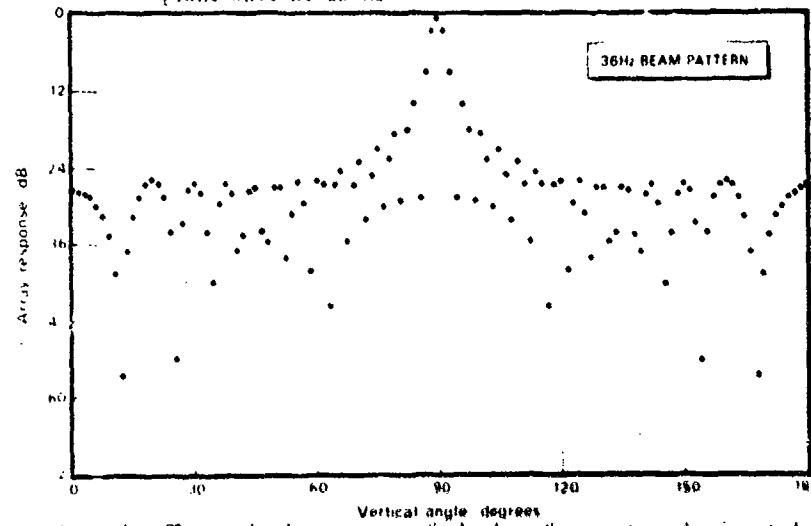


Fig. 4. Theoretical response of the beamformer to a horizontal plane wave at 36 Hz.

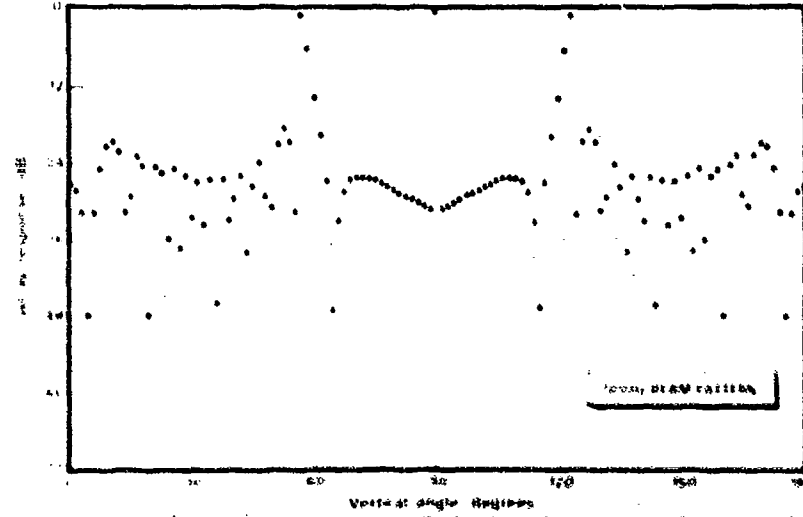


Fig. 5. Theoretical response of the beamformer to a horizontal plane wave at 100 Hz.

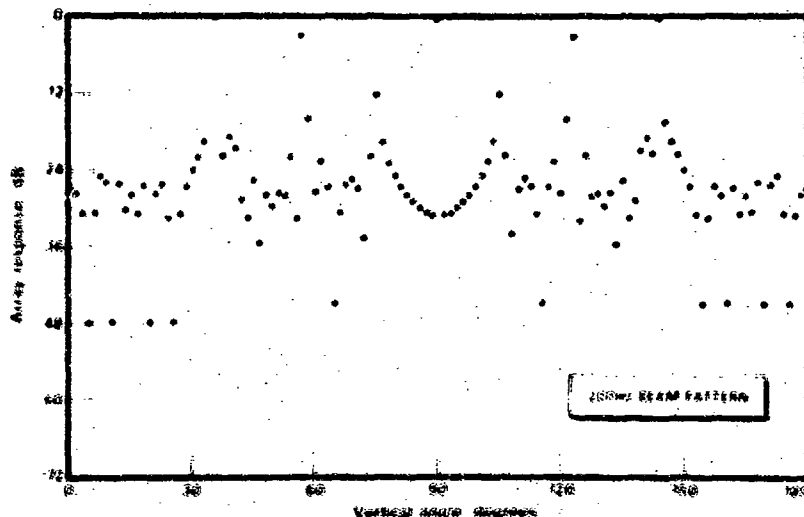


Fig. 6. Theoretical response of the beamformer to a horizontal plane wave at 300 Hz.

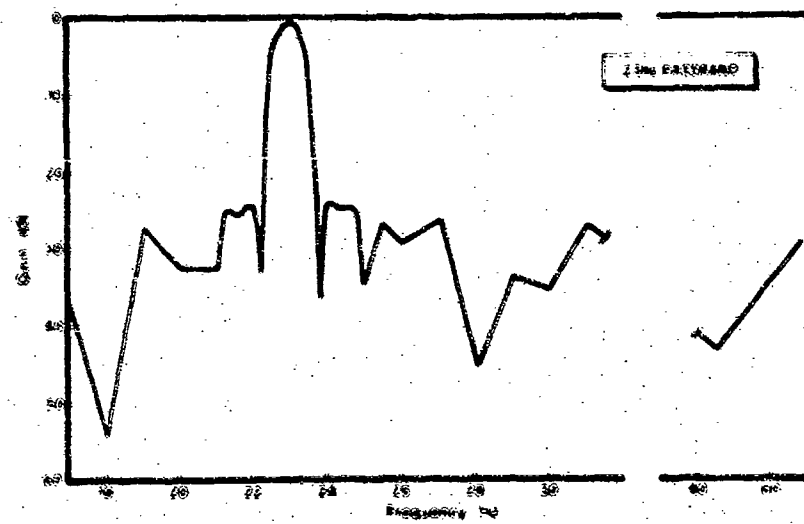


Fig. 7. Measured frequency response of the beamform bandpass filter at 30 Hz.

Histogram bins yielding 300 points in each histogram array. At this time the mean was calculated and the median, 10 percentile and 90 percentile bins determined. The histogram data was then condensed and stored on magnetic tape along with the median-mean-percentile arrays. Optional plots of both the median-mean-percentile vs. bin number and the histograms for each beam could be printed from these tapes. Plots and selected histograms were completed by individually selecting a sampling of these selected histogram plots generated across 16 certain regularly spaced

levels of the digital filter. Output gains talk in digital cables between the beamformer output and the decoder was identified as the cause. The data occurring at these values were rejected and the spaces filled by linear interpolation. Here, the quantization of the filter data varies from 0.2% to 0.9% as according to a specific algorithm and probability corrections for the following values were necessary after using 1, 1, 23 histogram bins. An example of an uncorrected and corrected histogram is shown in Fig. 8. All corrections to the histograms were

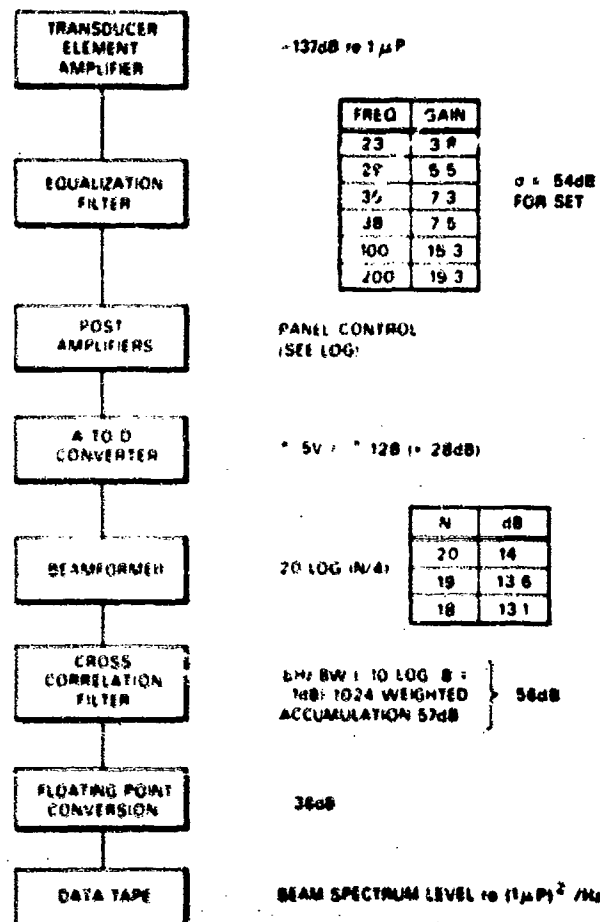


FIG. 8. System gain factors.

Programmed by night March 1974. A program was completed in April 1974 whereby the corrected autocorrelation data could be displayed by a line printer contour plotting routine. With this routine, up to five contour levels of any height may be selected with each level being represented by a different set of printer characters. These printer contour plots were useful in monitoring the data analysis. Two representative sets of contours have been plotted for inclusion in this report (Figs. 12 and 13).

The Appendix contains the plots of directional spectra for the data sets listed in Table II. For the noise sets, only the three lower frequencies are included. The ambiguities associated with the high grating lobes in spectra at 200 Hz are too severe to allow for meaningful interpretation. For the signal sets, one noise frequency plot is included with the two source frequency plots of the R tapes, only the three signal frequency sets are included for the P tapes.

DISCUSSION

There are two effects associated with the beamformer instrumentation which will affect

the interpretation of the data. The first of these is the apparent presence of common mode noise which was mentioned earlier. The evidence which gives rise to the assumption of the presence of such common mode noise lies in a careful examination of the directional plots associated with low background levels, particularly the noise runs of tapes labeled C and L. In all of these tapes, at all four frequencies, regardless of depth, there appears to be a strong signal precisely centered on the 90° beam. Although one might expect some one arrival to come in at precisely 90° at a particular depth, if there were such an arrival present at the deeper depths the angle would obviously be different for the rays as they crossed the sound channel axis at the shallower depths. This is not the case. Also, if there were truly a horizontal ray, one would expect to see at least a representative offset caused by the tilt angle on the array which was observed to vary up to 2 or 3 degrees during the experiment. There is no evidence of this displacement. The only logical explanation for this strong 90° beam is a signal which is common in phase in all elements. Because this effect occurs over all frequencies observed, the assumption has to be that it is also a broadband noise. The origin of this noise has not been identified to date.

In view of the appearance of this noise in the data, the 100 Hz results become particularly significant. Referring back to Fig. 5, one sees that the particular set of 1.5° beam sampling intervals which nearly matches the angular periodicity in the beam pattern, gives rise to a very low beam power output in the vicinity of the mean beam. This means that, for the data at 100 Hz, one can place a high confidence in the results around the central beam, since all of the common mode noise contamination will be concentrated in the 90° beam. Thus, it is the 100 Hz data which gives us the most significant clue as to the shape of the noise window as a function of depth. The disadvantage of the 100 Hz data, of course, is the presence of the second order grating lobes which limit the observation interval to a band of about ±15° about the horizontal. Thus, although the fine scale structure within the ±15° band is characterized by the 100 Hz plots, the lower frequency plots must be used to define the band in the upper levels of the ocean where the noise band exceeds the ±15° width.

Another effect of the instrumentation is the filling of the side lobes which obscures the correct interpretation of the directional spectrum for angles greatly removed from the horizontal direction. The mechanism whereby the side lobes are filled in is somewhat dubious. It is obvious that the directional response for the 24 Hz and 36 Hz plots do not approach the side lobe levels shown in the corresponding theoretical beam patterns of Figs. 1 and 4. In analyzing this effect, it

TABLE II
Comparison of Results of Calculations 21, 24, 46 and 48

ప్రాణికి విషాదం కలిగిన విషాదానికి అనుమతి దియాలి.

TABLE I
Traps, Frequency, Range, Wind, Range, Freq., Depth
Source No. (kHz) (kHz) (dB) (dB) (Hz) (m)

Source No.	Source Frequency		Depth (m)	Wind	Range (dB)	Freq. (Hz)	Depth (m)
	Low	High					
10012	* 19.7	89.6	2000	24.3	160 to 90	22.0	160
10015	* 19.6	69.7	1000	24.3	11 to 90	15.7	130
10017	* 19.7	108.3	74.3	17.1	15 to 100	16.0	23.3
10027	* 19.7	102.9	12.5	12.2 to 11.5	8.1	160	21.7

Source = Trap; * = range

TABLE II

Traps, Frequency, Range, Wind, Noise

Traps No.	Trap Number		Wind	Range (dB)	Filt Angle
	Low	High			
C1016	* 39.7	105.0	16.5	45 to 115	4 to 115
C1017	* 39.7	105.0	16.5	45 to 115	2 to 30
C1018	* 39.7	105.0	16.5	6 to 100	2 to 30
C1019	* 39.7	105.0	16.5	6 to 100	1.5 to 2.5°
C1020	* 39.7	105.0	16.5	6 to 100	2 to 30
C1021	* 39.7	105.0	16.5	6 to 100	2 to 30
G1016	* 39.7	105.0	16.5	45 to 115	No Data
G1017	* 39.7	105.0	16.5	45 to 115	No Data
G1018	* 39.7	105.0	16.5	45 to 115	No Data
G1019	* 39.7	105.0	16.5	45 to 115	No Data
G1020	* 39.7	105.0	16.5	45 to 115	No Data
G1021	* 39.7	105.0	16.5	45 to 115	No Data

Traps, Frequency, Range, Wind, Noise

TABLE III
B TRAPS - Sensitivity thru L.R.A.P.P System - 21 May 1974

Tran No.	Sensitivity & Element Amps (re 1uV)	Equalization Filters				Post Amp	Beam- former	Filter ($\sqrt{\text{Hz}}$)	A/D and Floating Pt. Conversion	TOTAL			
		F1	F2	F3	F4					F1	F2	F3	F4
B01	-137	3.8	5.5	7.5	15.3	20	11.6	56	-8	51.6	49.9	47.9	40.1
B02	-137	3.8	5.5	7.5	15.3	20	13.6	56	-8	51.6	49.9	47.9	40.1
B03	-137	3.8	5.5	7.5	15.3	25	13.6	56	-8	56.6	54.9	51.9	35.1
B04	-137	3.8	5.5	7.5	15.3	25	13.6	56	-8	56.6	54.9	51.9	35.1
B05	-137	3.8	5.5	7.5	15.3	25	13.6	56	-8	56.6	54.9	51.9	35.1
B06	-137	3.8	5.5	7.5	15.3	20	14	56	-8	51.2	49.5	47.5	39.7
B07	-137	3.8	5.5	7.5	15.3	20	14	56	-8	51.2	49.5	47.5	39.7
B08	-137	3.8	5.5	7.5	15.3	20	14	56	-8	51.2	49.5	47.5	39.7
B09	-137	3.8	5.5	7.5	15.3	25	14	56	-8	46.2	44.5	42.2	34.7
B10	-137	3.8	5.5	7.5	15.3	25	14	56	-8	46.2	44.5	42.2	34.7
B11	-137	3.8	5.5	7.5	15.3	25	14	56	-8	46.2	44.5	42.2	34.7
B12	-137	3.8	5.5	7.5	15.3	25	13.6	56	-8	46.2	44.5	42.2	34.7
B13	-137	3.8	5.5	7.5	15.3	25	14	56	-8	46.2	44.5	42.3	34.7
B14	-137	3.8	5.5	7.5	15.3	25	14	56	-8	46.2	44.5	42.3	34.7
B15	-137	3.8	5.5	7.5	15.3	25	14	56	-8	46.2	44.5	42.3	34.7
B16	-137	3.8	5.5	7.5	15.3	25	14	56	-8	46.2	44.5	42.3	34.7
B17	-137	3.8	5.5	7.5	15.3	25	14	56	-8	46.2	44.5	42.3	34.7
B18	-137	3.8	5.5	7.5	15.3	25	14	56	-8	46.2	44.5	42.3	34.7

TABLE III (Con't)
C, D and E TAPES - Sensitivity thru LRAPP System 21 May 1974

Tape No.	Sensitivity & Element Amps (re 1 μ P)	Equalization Filters				Post Amp	Beam- former	Filter (V 1/2)	A/D & Floating Pt. Conversion	TOTAL			
		F1	F2	F3	F4					F1	F2	F3	F4
C01	-137	3.8	7.3	15.3	19.3	20	14	56	-8	51.2	47.7	39.7	35.7
C02	-137	3.8	7.3	15.3	19.3	20	14	56	-8	51.2	47.7	39.7	35.7
C03	-137	3.8	7.3	15.3	19.3	20	14	56	-8	51.2	47.7	39.7	35.7
C04	-137	3.8	7.3	15.3	19.3	20	14	56	-8	51.2	47.7	39.7	35.7
C05	-137	3.8	7.3	15.3	19.3	20	14	56	-8	51.2	47.7	39.7	35.7
D01	-137	5.5	7.3	7.5	15.3	20	14	56	-8	49.5	47.1	47.5	39.7
D03	-137	5.5	7.3	7.5	15.3	20	13.1	56	-8	50.4	48.6	48.4	40.6
D05	-137	5.5	7.3	7.5	15.3	25	14	56	-8	49.5	47.7	47.5	39.7
D07	-137	5.5	7.3	7.5	15.3	25	14	56	-8	49.5	47.7	47.5	39.7
E01	-137	3.8	7.3	15.3	19.3	20	14	56	-8	51.2	47.7	39.7	35.7
E02	-137	3.8	7.3	15.3	19.3	20	14	56	-8	51.2	47.7	39.7	35.7
E03	-137	3.8	7.3	15.3	19.3	20	14	56	-8	51.2	47.7	39.7	35.7
E04	-137	3.8	7.3	15.3	19.3	20	14	56	-8	51.2	47.7	39.7	35.7
E05	-137	3.8	7.3	15.3	19.3	20	14	56	-8	51.2	47.7	39.7	35.7
E06	-137	3.8	7.3	15.3	19.3	15	14	56	-8	56.2	51.7	44.7	40.7
E07	-137	3.8	7.3	15.3	19.3	20	14	56	-8	51.2	47.7	39.7	35.7

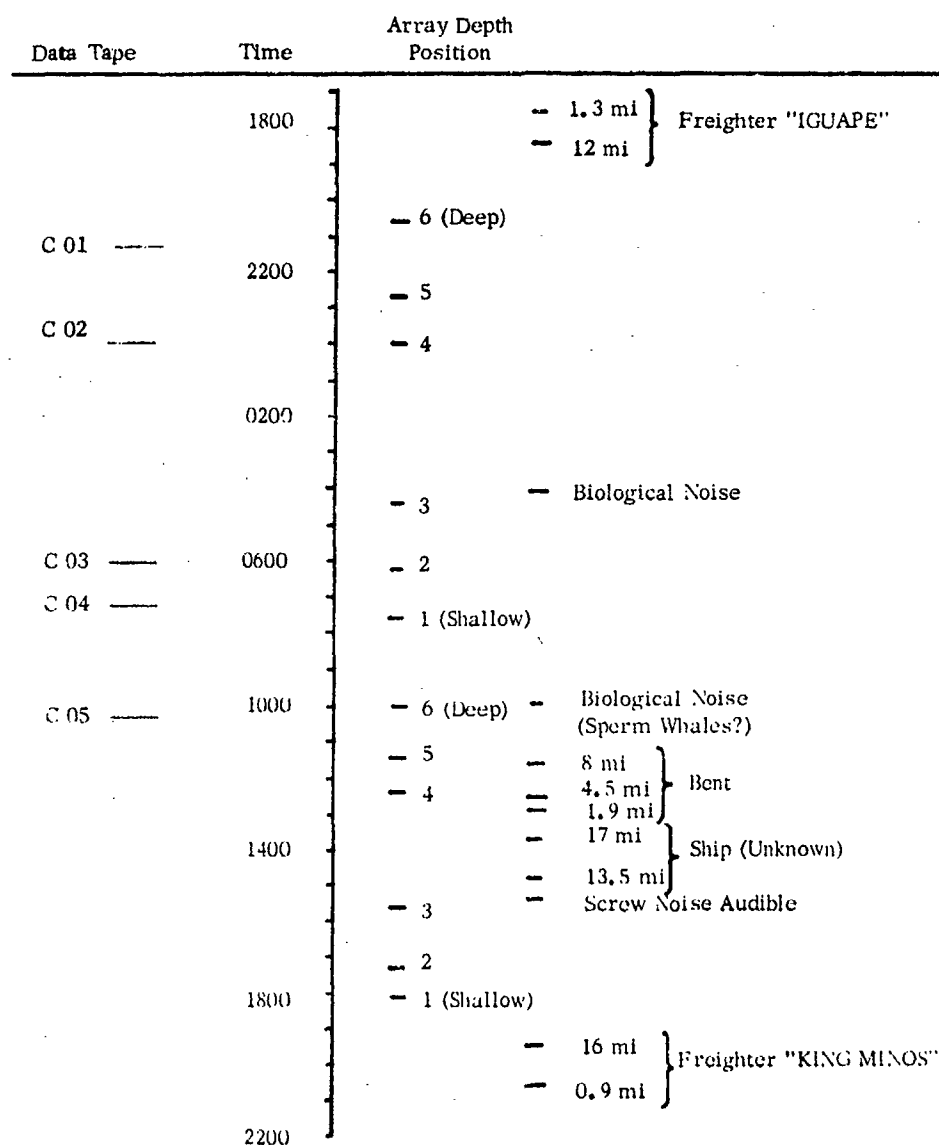


Fig. 9. Local ship traffic near FLIP during 5-6 September 1973 noise period.

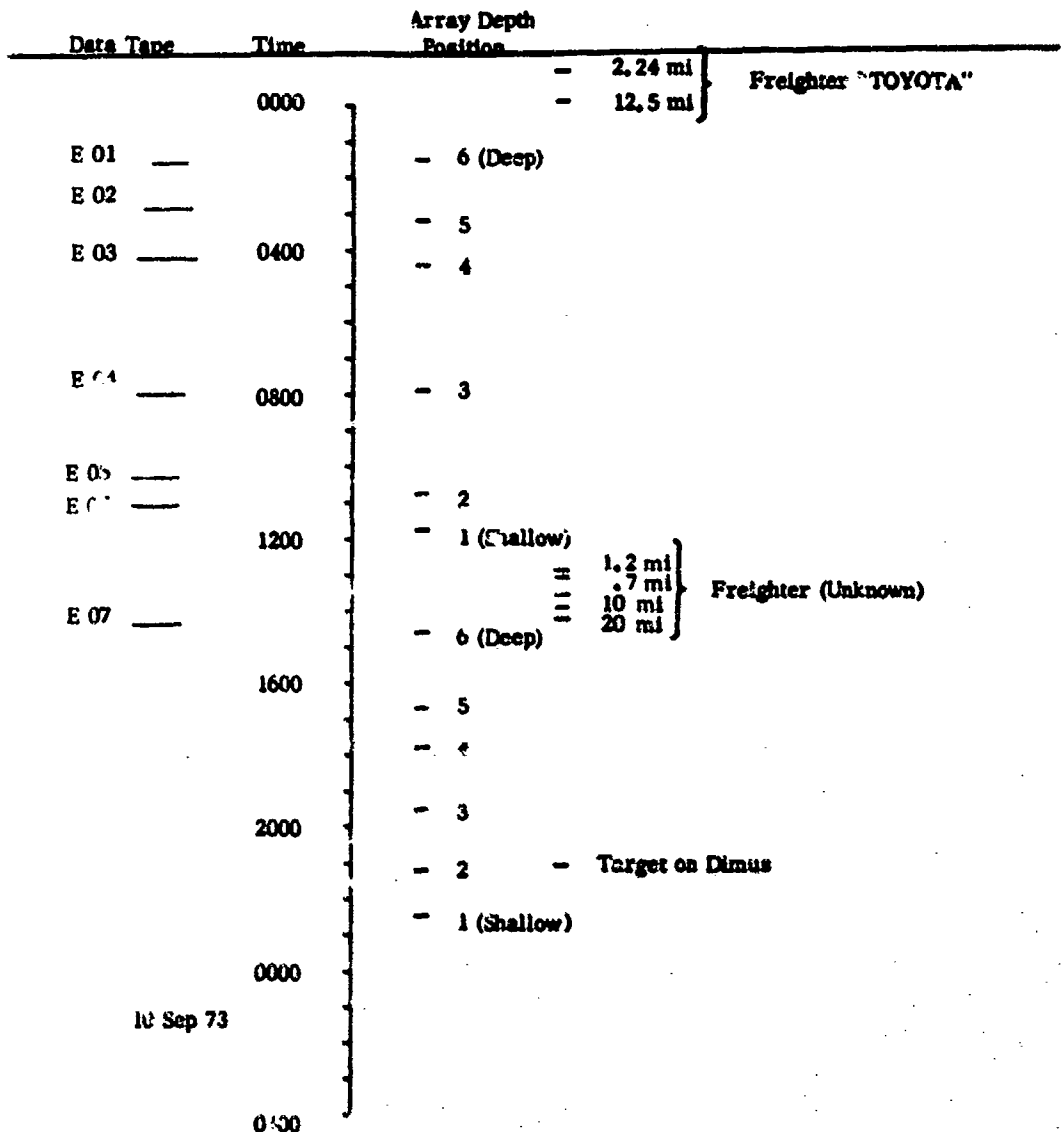


Fig. 10. Local ship traffic near FLIP during 8-9 September 1973 noise period.

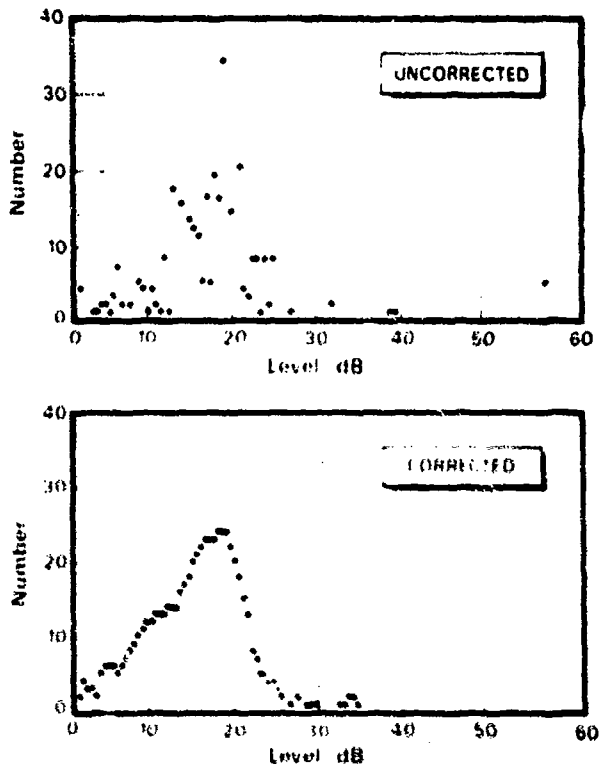


Fig. 11. Histogram correction example.

is important to recall that the beamforming is done on a broad band basis within the beamformer and that the narrow-band filtering is accomplished after the summation process.

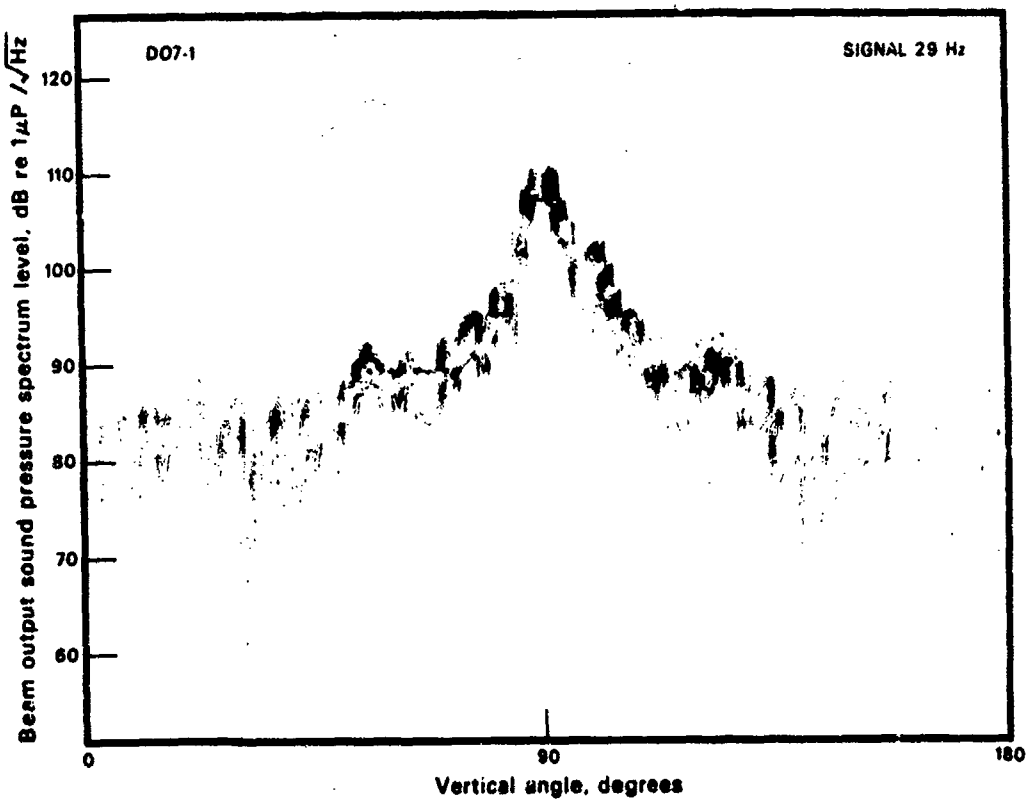
The full bandwidth of something greater than 500 Hz of noise will have an average side lobe level corresponding to approximately the directivity index of the array or about -13 dB. This can be thought of as being the effects of the power which feeds in through the high frequency secondary lobes which, because they are frequency dependent, will have essentially a uniform distribution over the angular aperture. The total power occurring in the side lobe region then will be roughly determined by the full band power reduced by the directivity index. For noise input of one volt rms with a total bandwidth of 500 Hz, the side lobe level would be -13 dB. If we consider the noise level in the 0.8 Hz band of 23 Hz from a broadband input of 1-volt rms it will be lower by the ratio of 0.8 to 500 Hz and also by the -13 dB equalization gain difference for a total level of -13 dB, and -30 dB with respect to the broadband side lobe level. The task of the narrow-band filter in the beamformer output is

then to separate the noise spectrum at 23 Hz from the rest of the broadband noise. The filter response of this narrow-band filter, shown in Fig. 7, indicates that a level of about -40 dB is representative of the skirts beyond the immediate vicinity of the pass band, thus the wideband noise in the beamformer side lobe region is suppressed by 40 dB placing it approximately -10 dB below the beam response at 23 Hz.

In the propagation runs with high signal-to-noise ratios, the beamformer is subjected to an input spectrum which contains only a few line components. For this case we do observe the beamformer side lobes to a much greater depth than the noise case. This feed through of out-of-band side lobe energy is quite evident in some of the propagation run tapes where two different frequency signals are present. For example, in the contour plot of tape D07 (Fig. 12) the two secondary lobes appearing in the 104 Hz plot (frequency four) show up in the three lower frequencies as bumps in the side lobe distribution. These are particularly evident in frequency two, 36 Hz, which was out of the band of the two other signal frequencies.

Further evidence of the fact that the side lobe energy is due to frequencies out of the filter band is to be seen in the contour plots. For example, in the contour plot for noise tape D01 (Fig. 13), frequency one (23 Hz), shows that in the side lobe region there are many places where the distribution is much narrower than that in the main beam. In the main beam one would expect to see a Rayleigh distribution which is roughly what the contours correspond to at that point. If the side lobe energy were truly associated with the energy in the 23 Hz band, it too would be expected to have a Rayleigh distribution. However, if it were a composite of frequencies outside of the band, then the number of degrees of freedom for each sample would be significantly higher and as a result the distribution for any one sample will be much narrower and the contours will converge in these regions as they appear to in this plot.

Estimates of the directional noise spectrum for the lower three frequencies, 23, 36, and 104 Hz are shown in Fig. 14. Perhaps the most reliable shape is that associated with the 104 Hz curve. The 104 Hz beam pattern is narrow enough to resolve the edges of the noise distribution which appears to have a very sharp edge to the directional spectrum. At the deepest depth, the curve shows a narrow directional spectrum with most of the energy confined to the region near the horizontal, the next step above the critical depth still shows a narrow spectrum but with an increase of 4 dB in level. As the array is raised progressively higher this noise distribution spreads but retains a very flat top distribution with no indication of a horizontal null and there is only a slight



Figs. 12a-12d. Contour plots of the histogram distributions for tape D07.

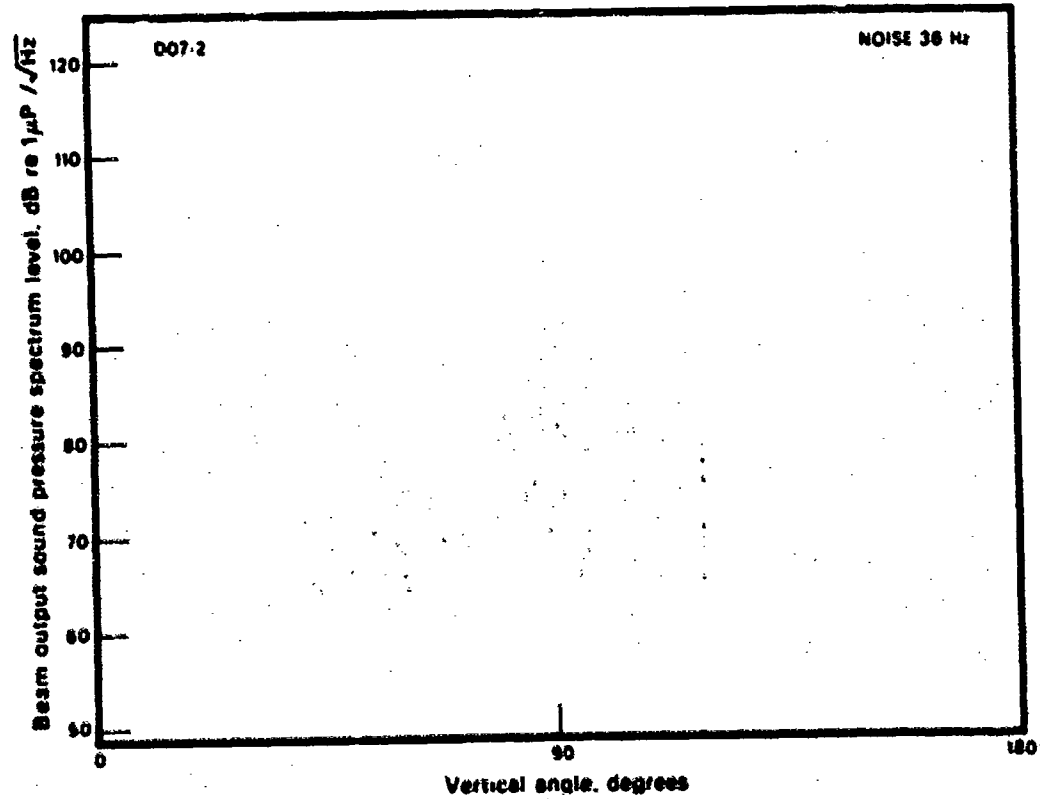


Fig. 12b

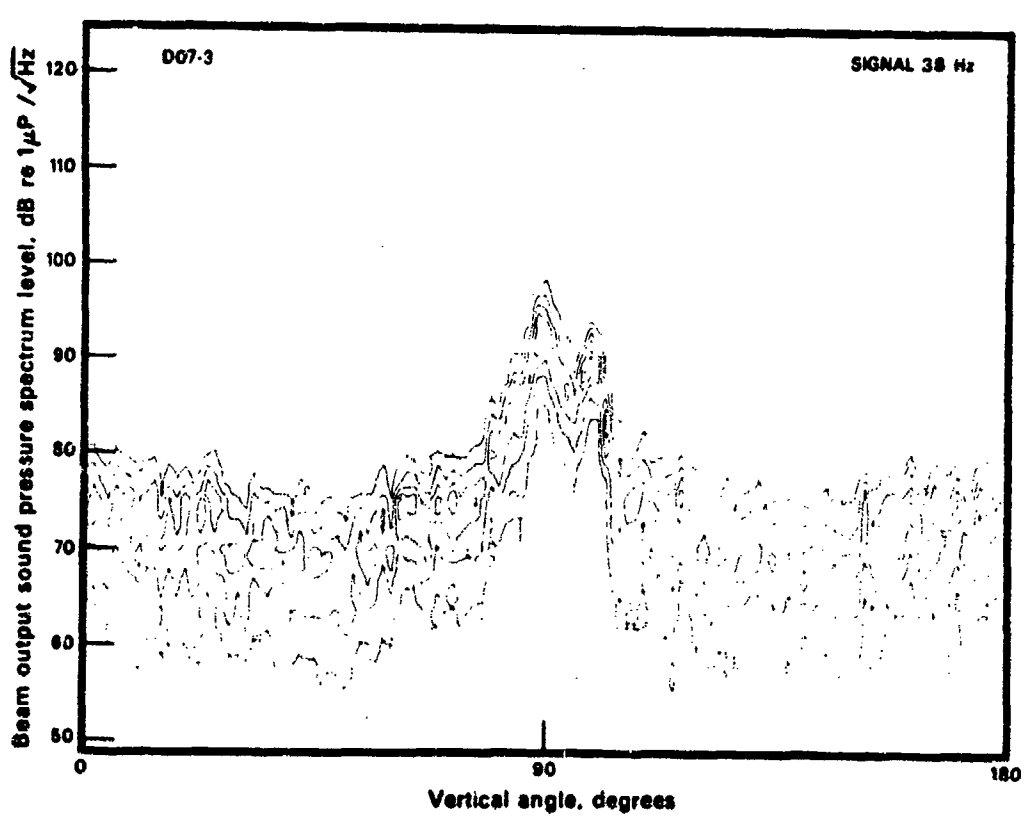


Fig. 12c

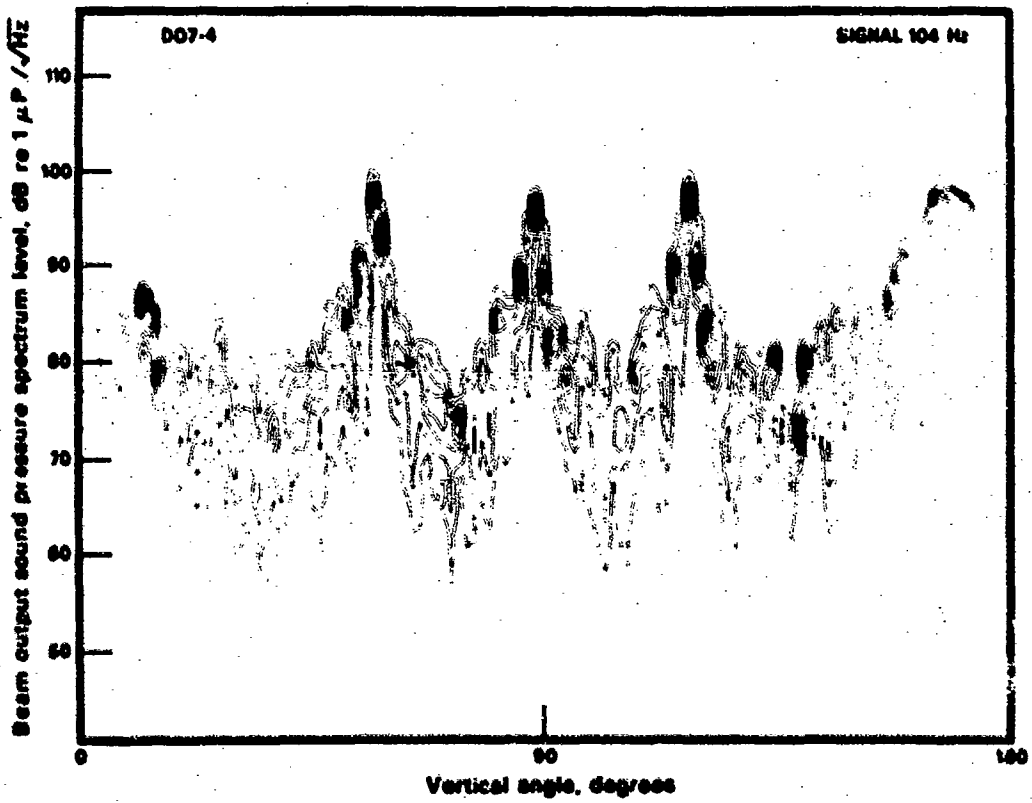
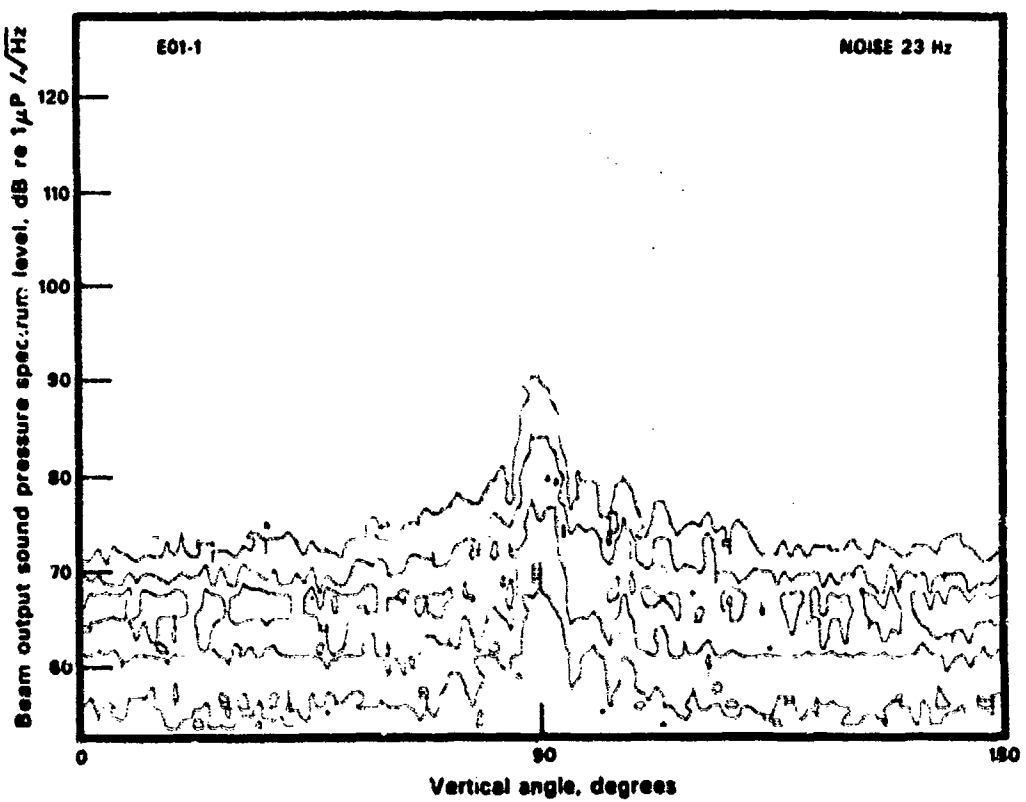


Fig. 12d



Figs. 13a-13c. Contour plots of the histogram distributions for tape E01.

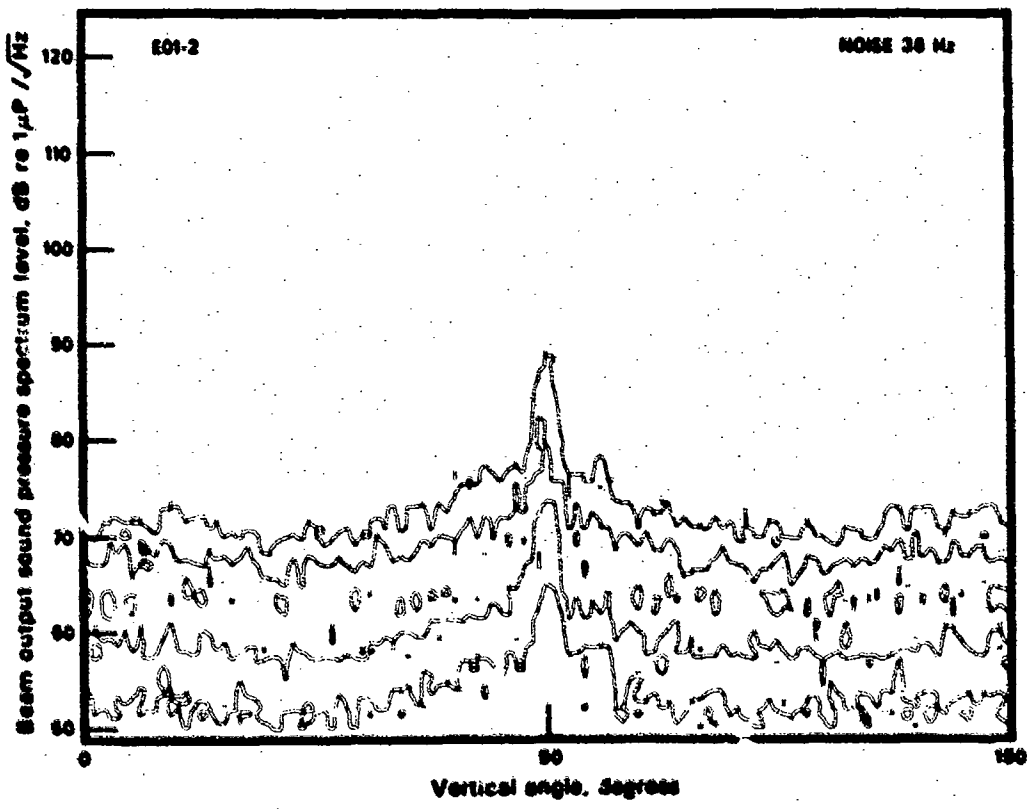


FIG. 13b.

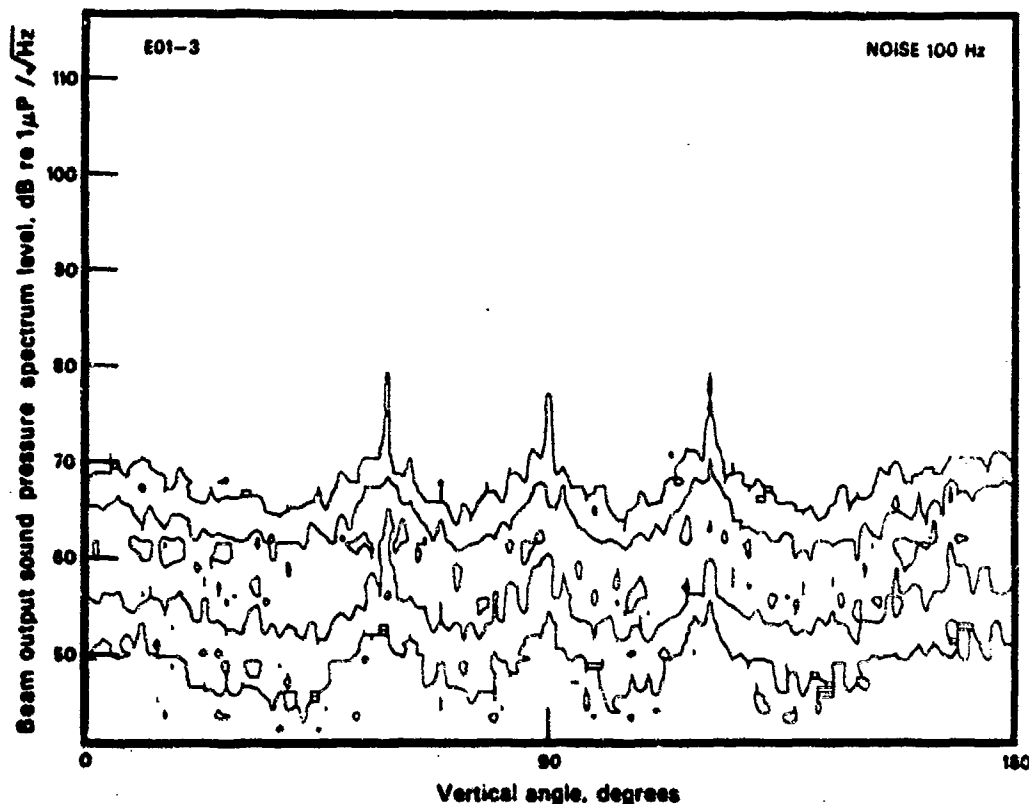


Fig. 13c

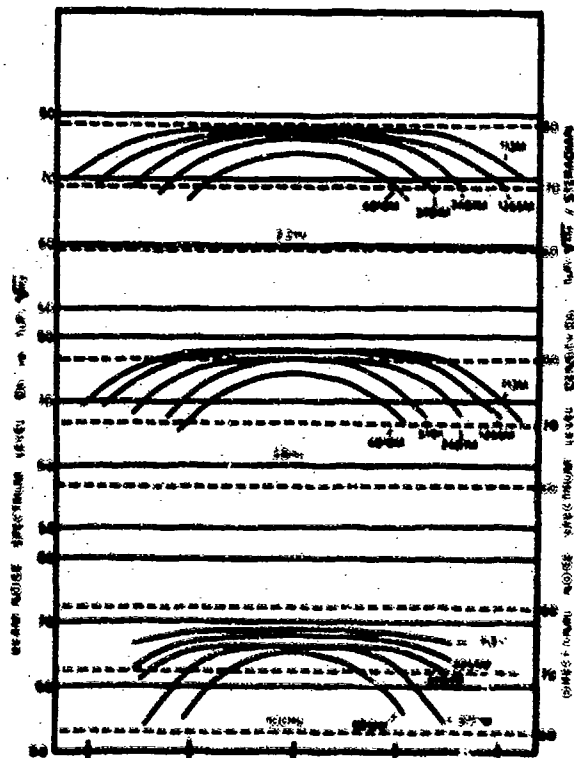


Fig. 14. Estimates of the directional noise spectrum for 25, 38 and 100 Hz.

Increase in the actual total noise power as a function of depth above the critical depth. For the two lower frequencies, 25 and 38 Hz, the curves associated with the two lowest steps are conjectural in nature and thus are dotted in. The 25 and 38 Hz directional spectra are severely obscured by the common mode noise which spreads over the broader beam width at these two frequencies. It has been assumed in drawing these arrays that they are similar to those of the 100 Hz curve which was clearly resolved by the filter. The shoulders of the square top noise distribution at the upper depths, however, do appear as a spreading of the directional spectrum for these two lower frequencies and more reliance may be placed on these upper level values. The side lobe regions outside of this main distribution lobe must be considered to be indeterminate in these experiments because they have been obscured by the previously mentioned filter leakage.

One word of caution should be voiced at this point, that is that the data accumulated here consists only of two sets of depth measurements, each represented by 10-minute samples of noise and in no way should this be construed to be anything other than a gross estimate of the noise structure. The structure is extremely variable, data from the same depth on two different runs differs by as much as 5 dB in average level and note

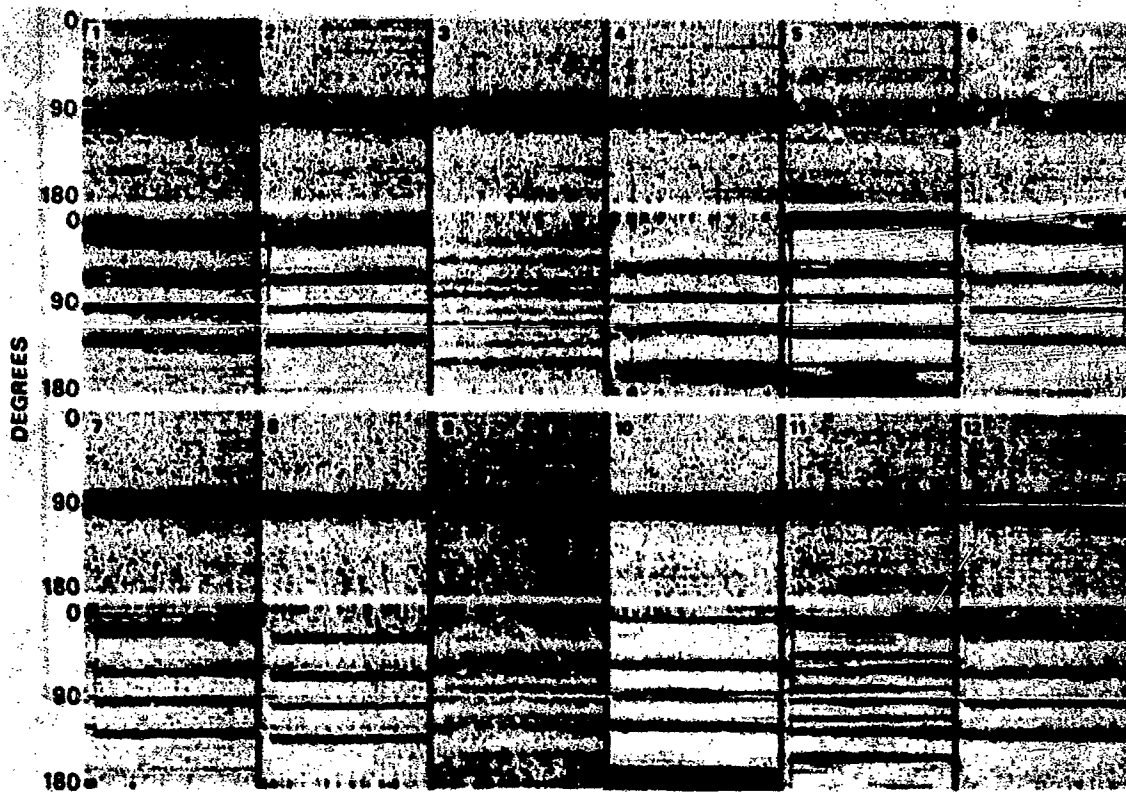


Fig. 15. Time-bearing intensity records which include the D05 and D07 directional spectra samples of signal transmissions.

than that in the detailed structure. The oceanic noise in the low frequency region cannot be considered stationary on a 10-minute or even 10-hour time scale.

The B and D tapes were taken during propagation runs with sources at two and sometimes three frequencies. Two different depths are associated with these runs, one depth with the center of the array at 713 meters, near the axis of the sound channel and the other just above the critical depth width the array center at 3781 meters. The directional arrivals are clearly shown in these plots. Another word of caution to be exercised in interpreting the data is in order, particularly for the 713 meter 100 Hz plots. The two arrival paths in this case are nearly exactly spaced on the spacing of the second order grating responses and the up and downcoming paths are superimposed on each other in these plots. Thus, what appears to be a spreading of the energy may merely be the superposition of the up and down rays at not quite the second order lobe spacing. In the case of the deep array the angular separation is much less, so close as a matter

of fact that for the low frequency end, the rays are not resolved by the beam pattern; however, at 100 Hz they can be seen to be separate. Significant changes in the distribution of energy between the up and down bundles can be seen from tape to tape. At the 100 Hz frequency the arrival ray bundle is in many cases spread out broader than the 1.5 resolution of the 100 Hz beam pattern.

Graphical intensity vs. vertical angle and time recordings were made during the experiment. A sequence of sections of such a record is shown in Fig. 15. Two of the tape directional spectra, D05 and D07, were taken during this sequence. D05 corresponds to Record #1 and D07 corresponds to Record #10. It is apparent that the average spectra plotted do not fully represent the complexity of the propagation path; there is a considerable time variability in both the direction and amplitude of the arrivals of Fig. 15.

The low frequency envelope spectra of these signal arrivals will be the subject of a future analysis and report.

ACKNOWLEDGMENT

This paper represents results of research sponsored by the Office of Naval Research.

REFERENCES

1. McDonough, R.N., Maximum-Entropy Spatial Processing of Array Data, NPL-U-85/73. Accepted for Publication in December 1974 issue Geophysics.

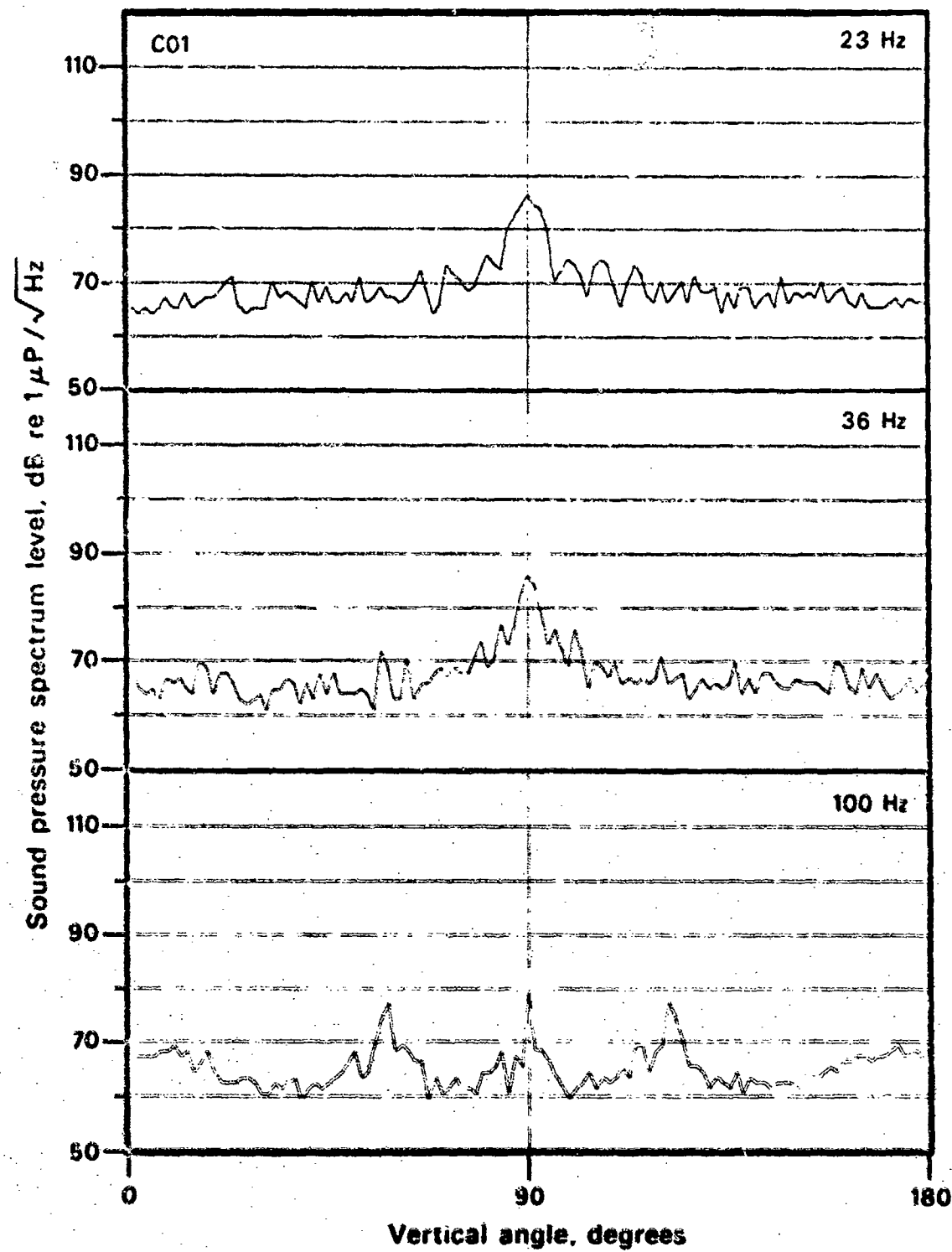
2. McDonough, R.N., Spectrum Restoration for Uniformly-Spaced Arrays, NPL-U-41/74 Submitted to J.Acoust.Soc.Am.
3. A complete description of the LRAPP beamformer is given in NPL-TM-236.

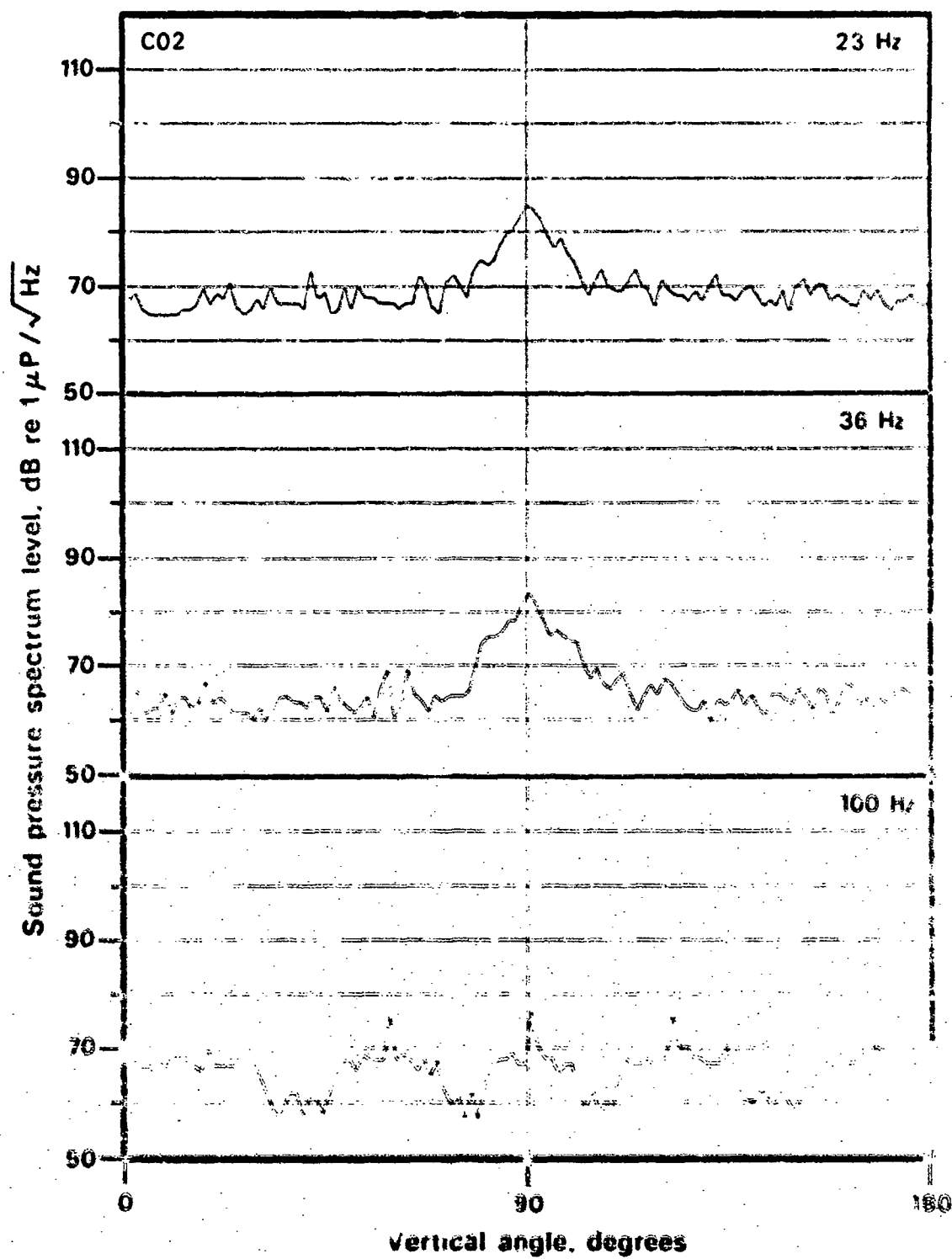
APPENDIX

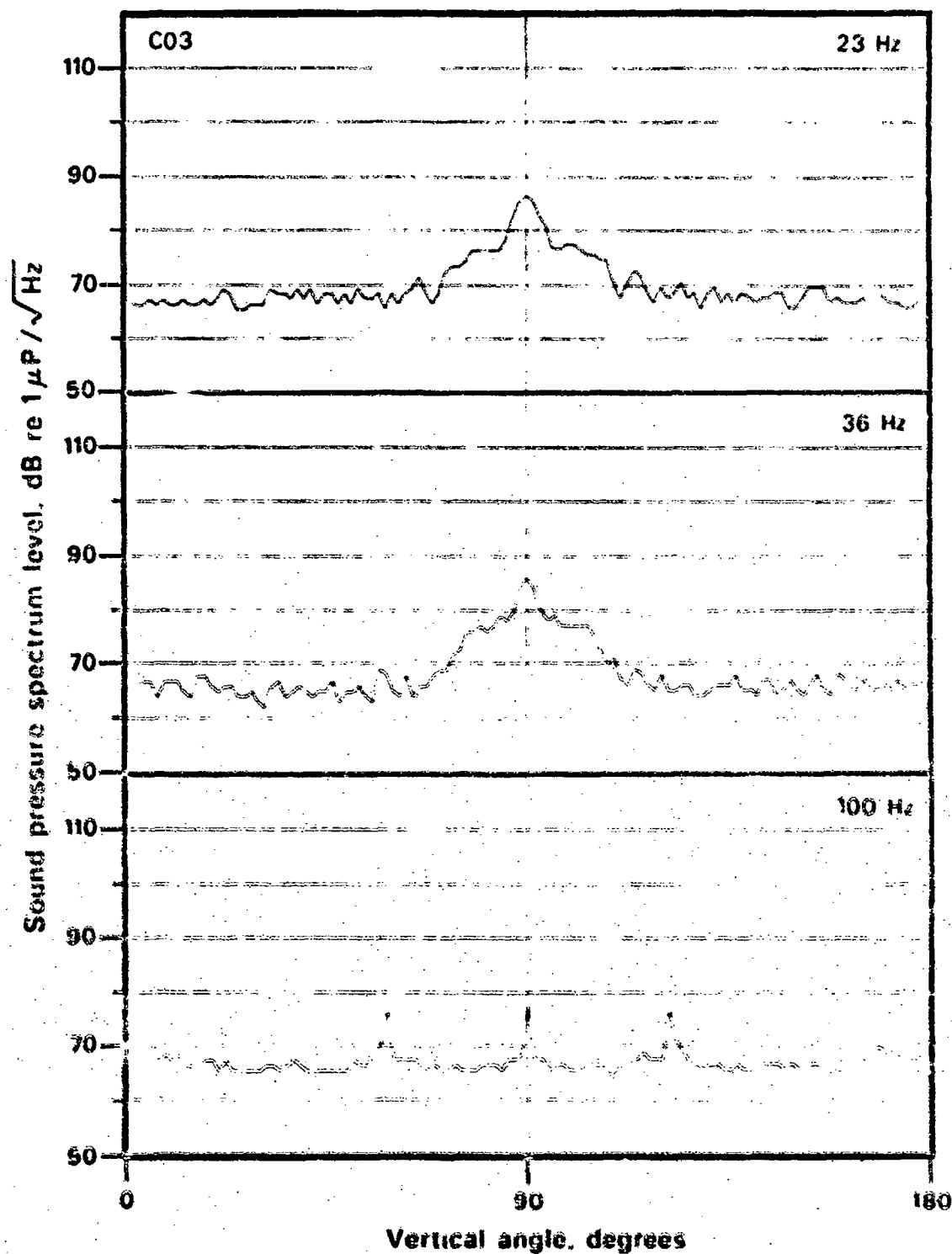
Directional spectra for the B, C, D and E tapes are included. Records are in an Alpha numeric tape sequence.

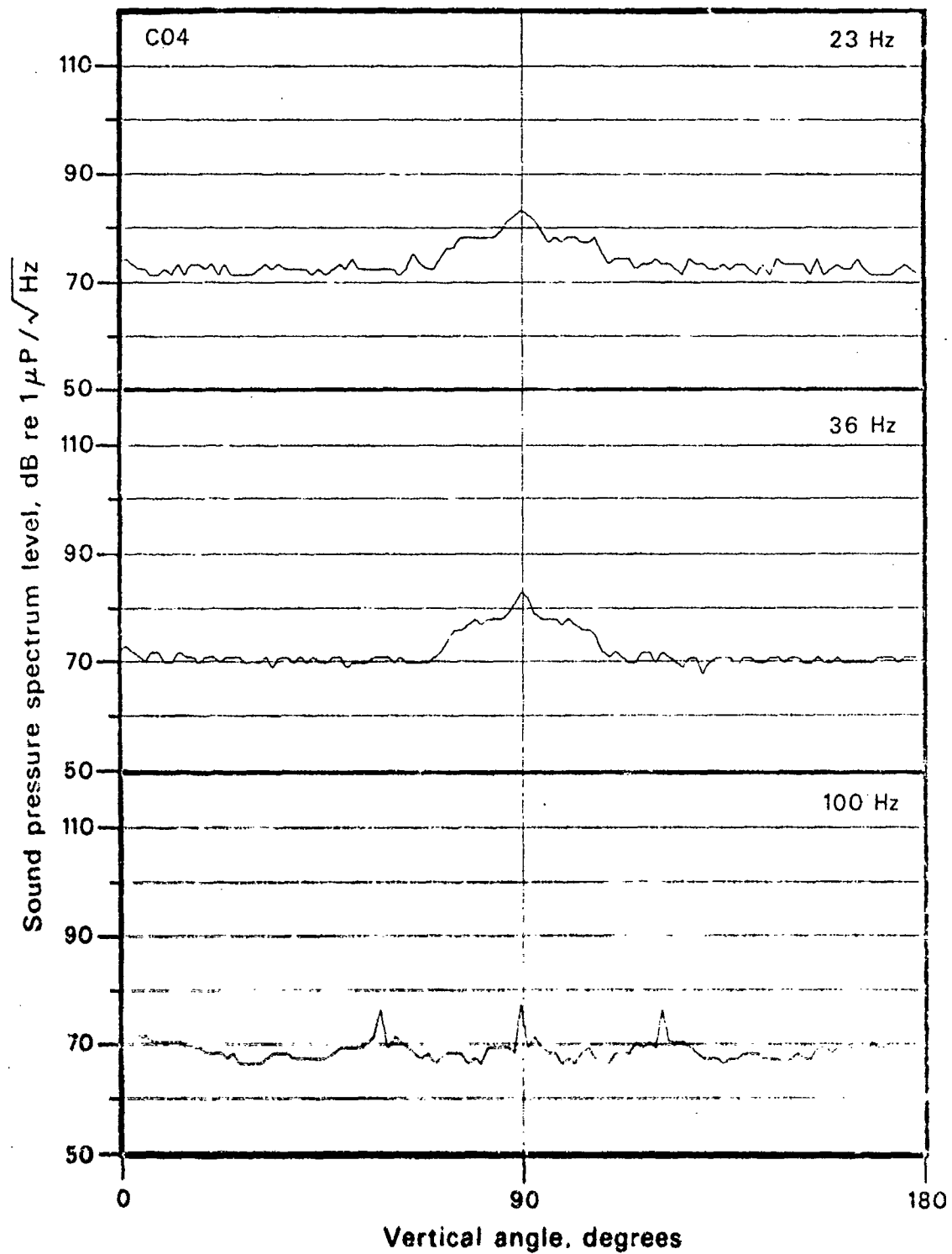
Anderson

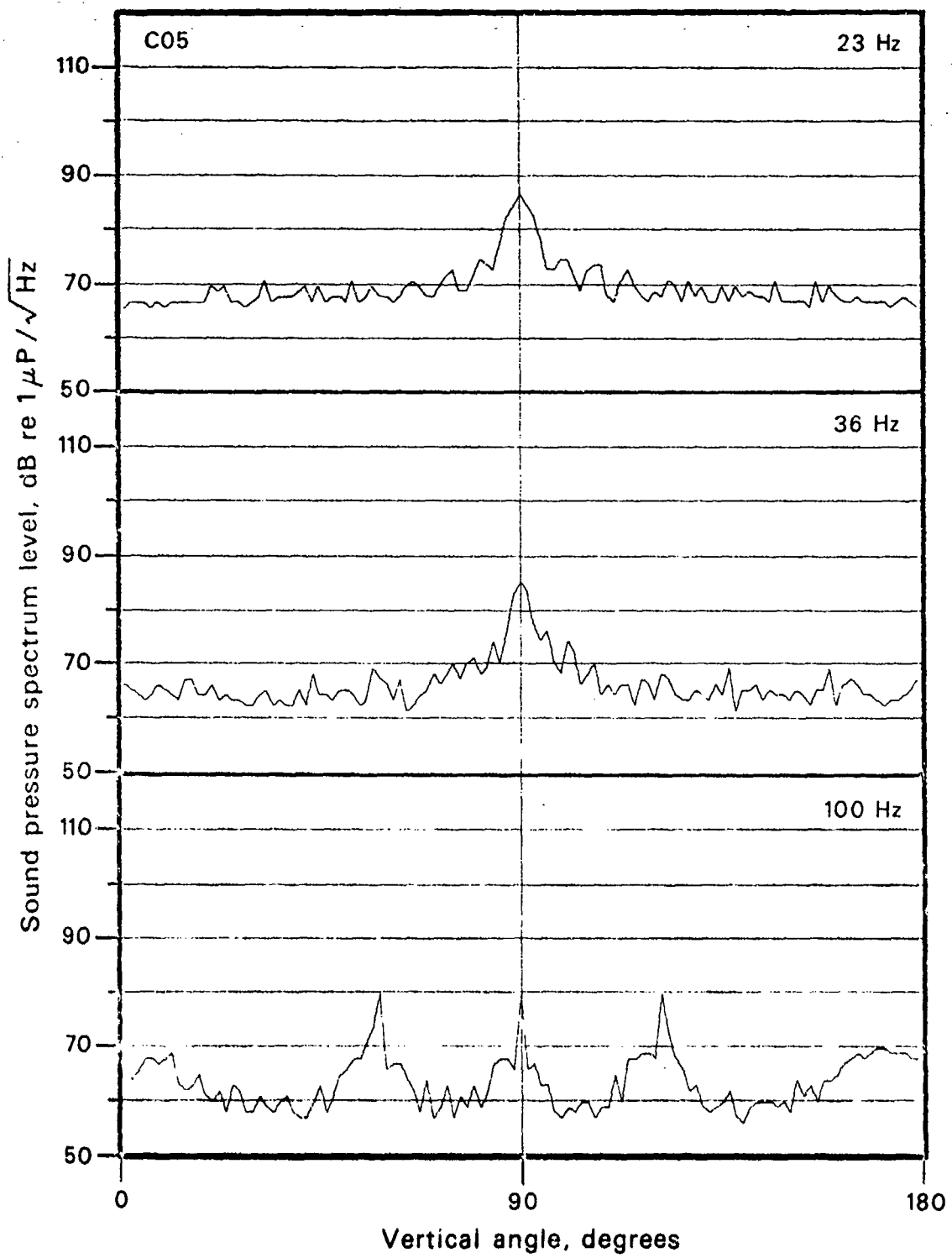
MPL-53/74

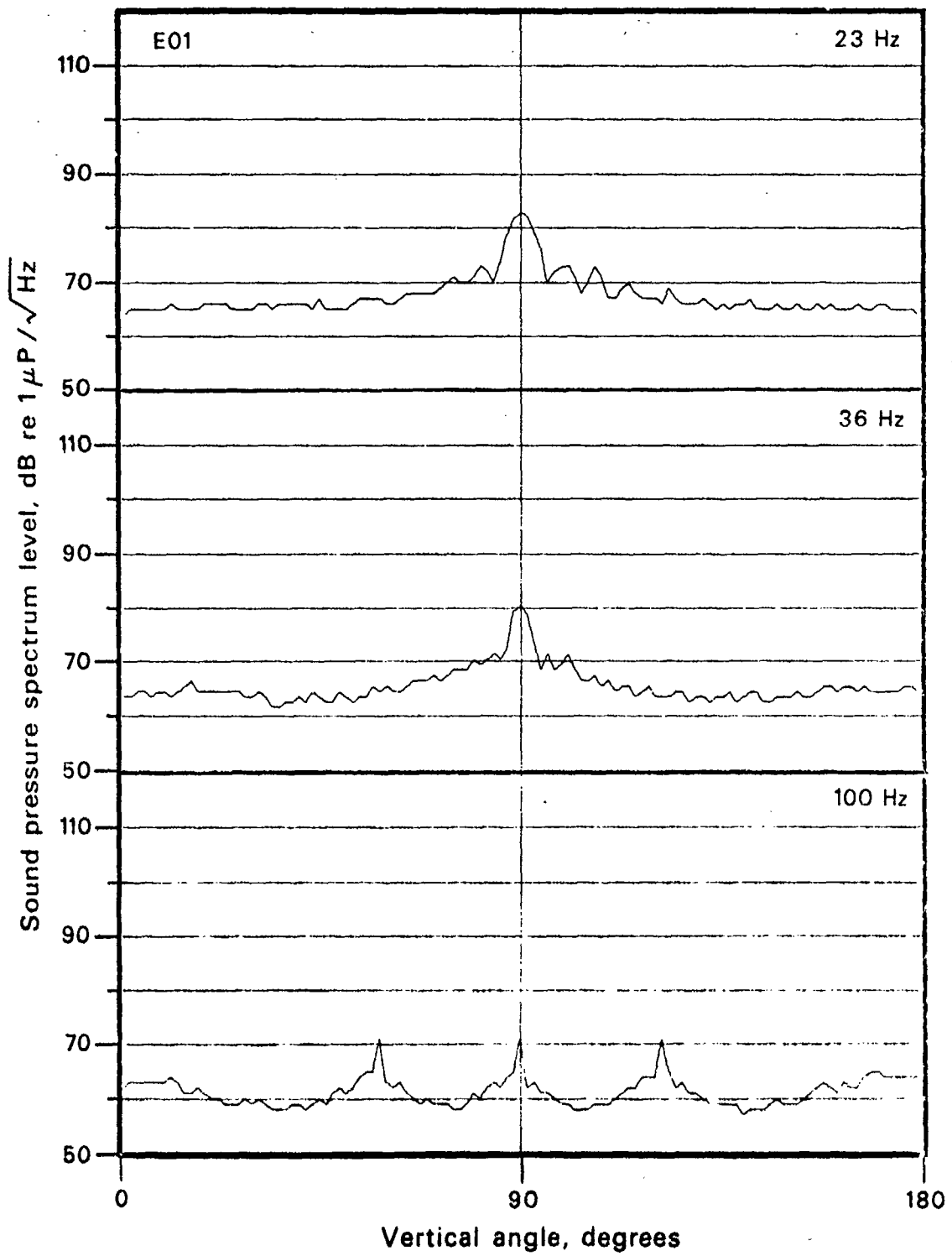


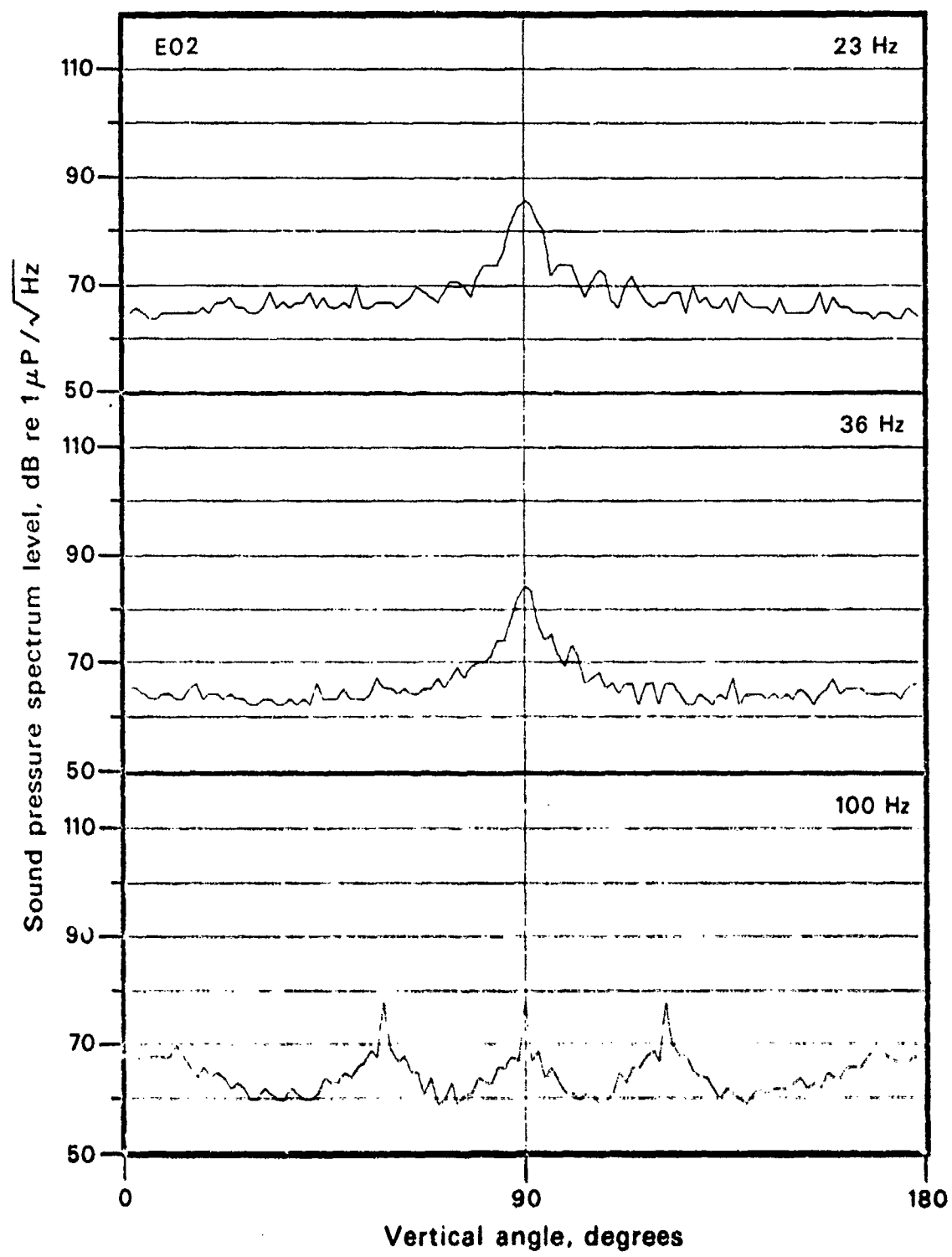


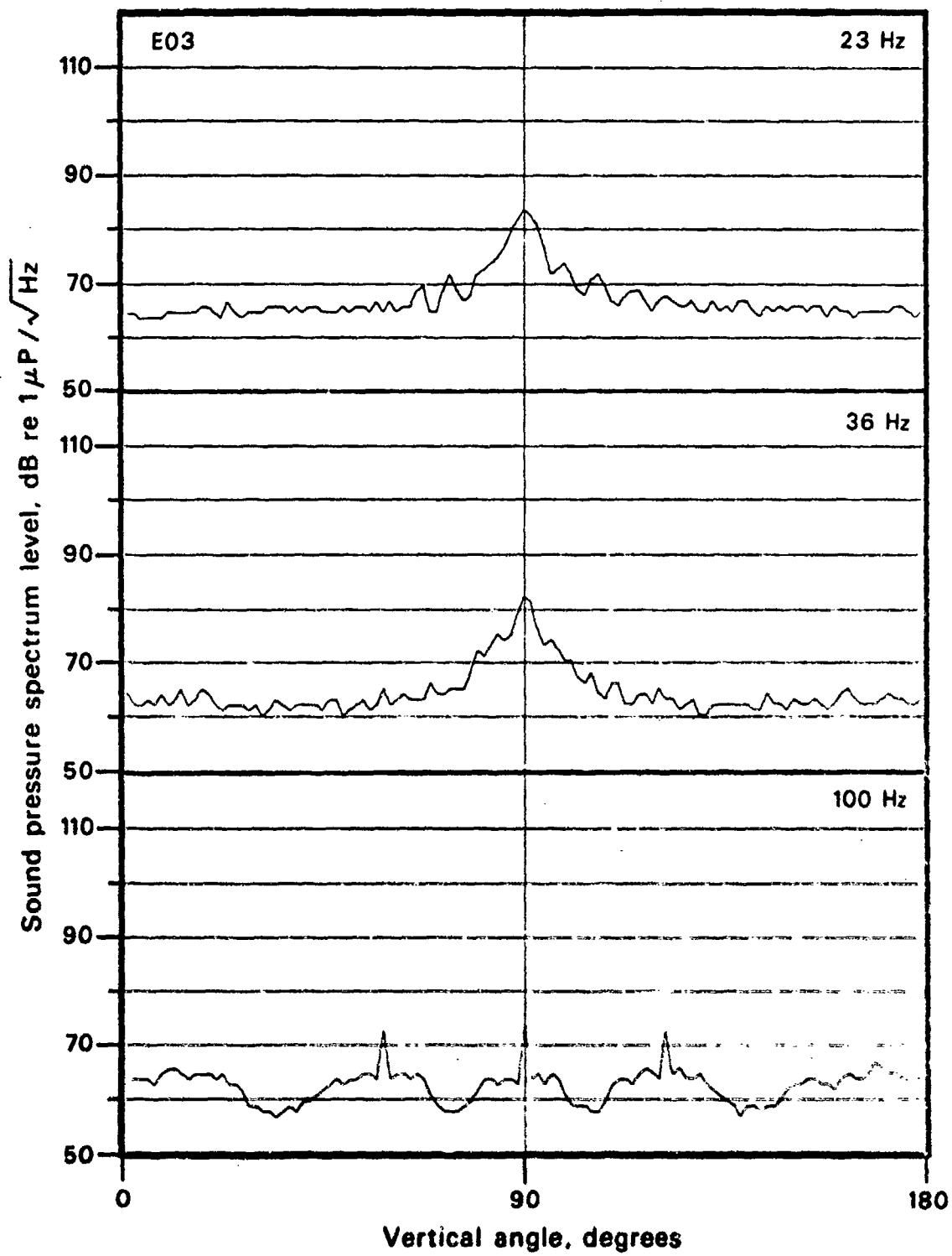


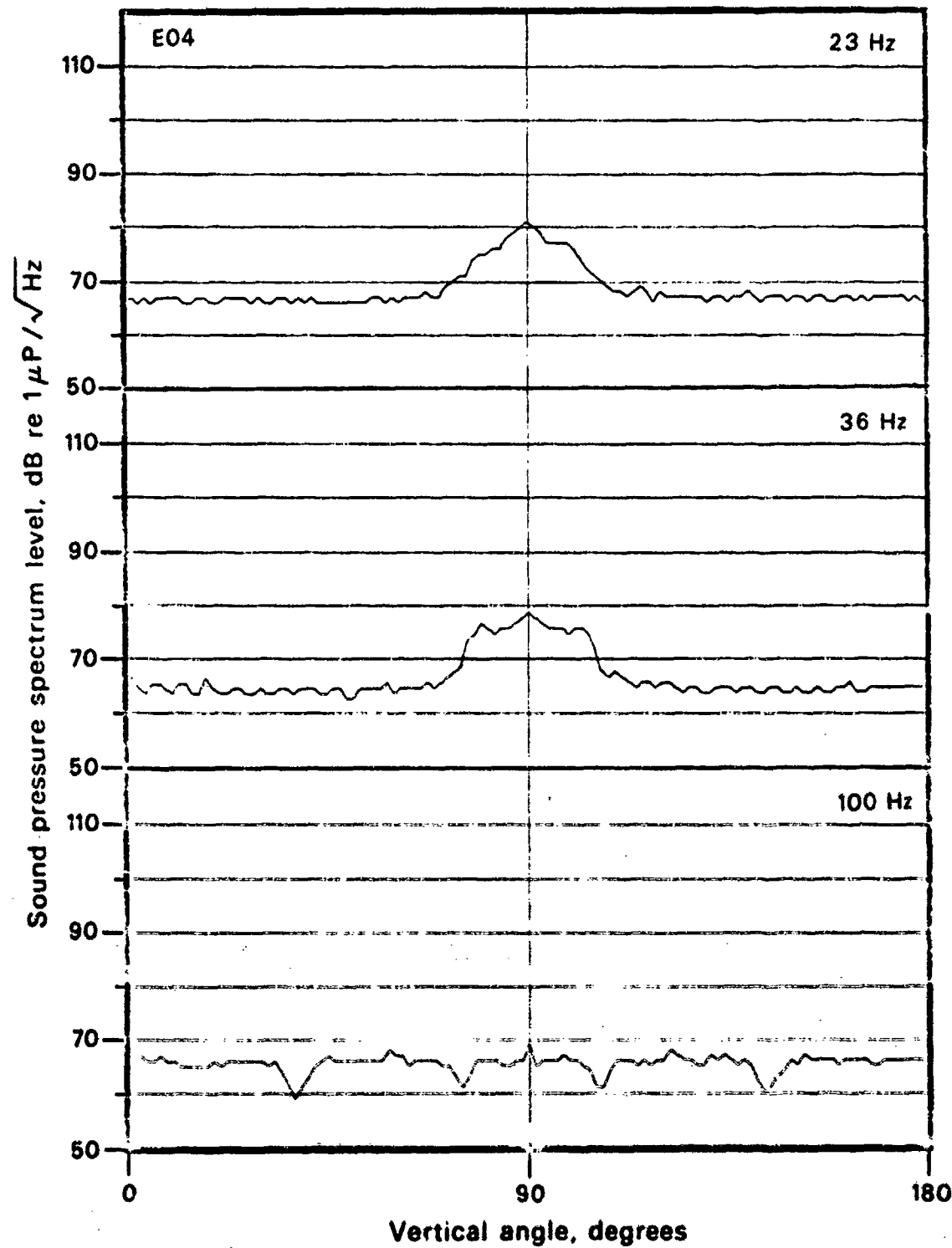


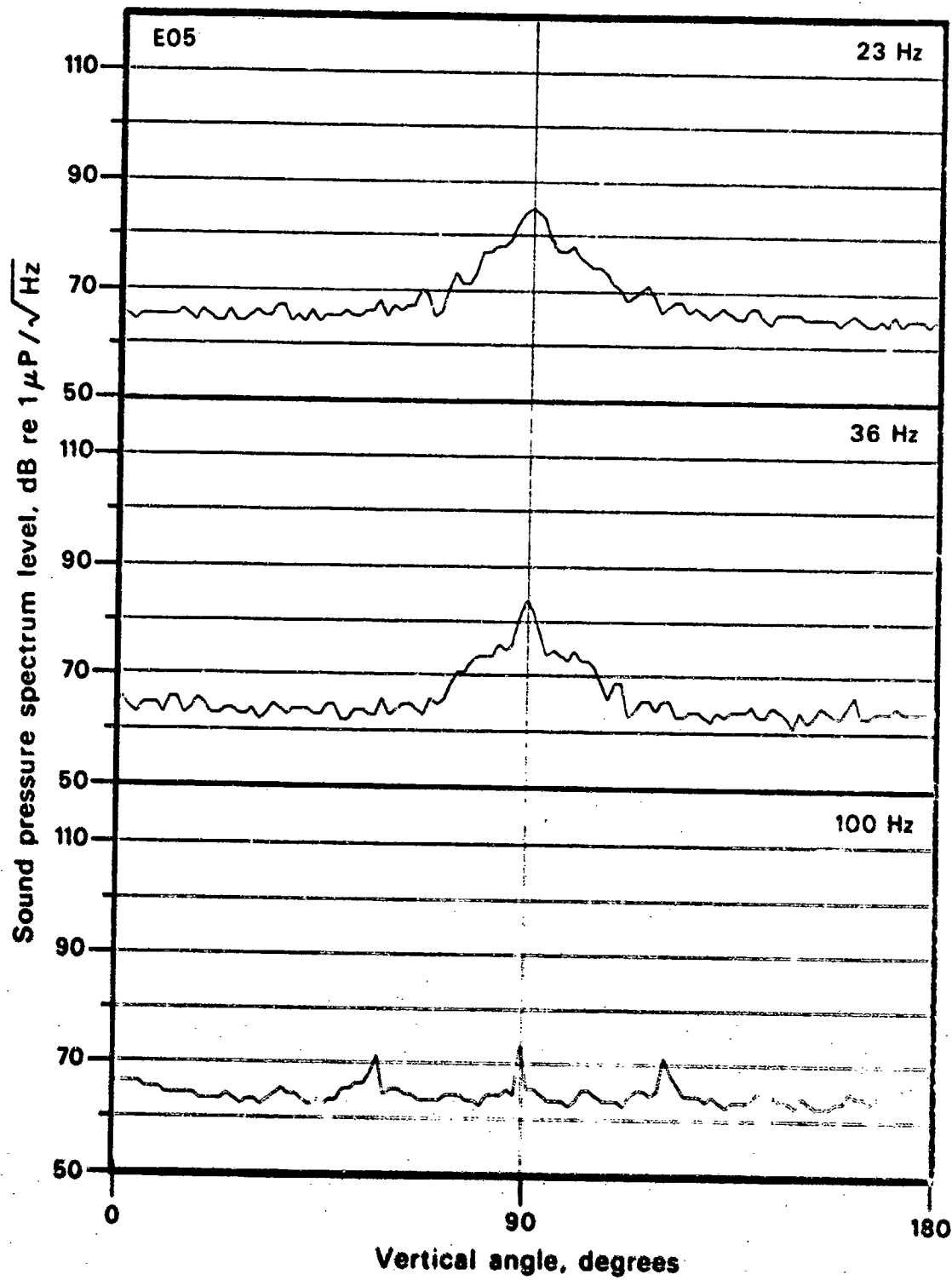


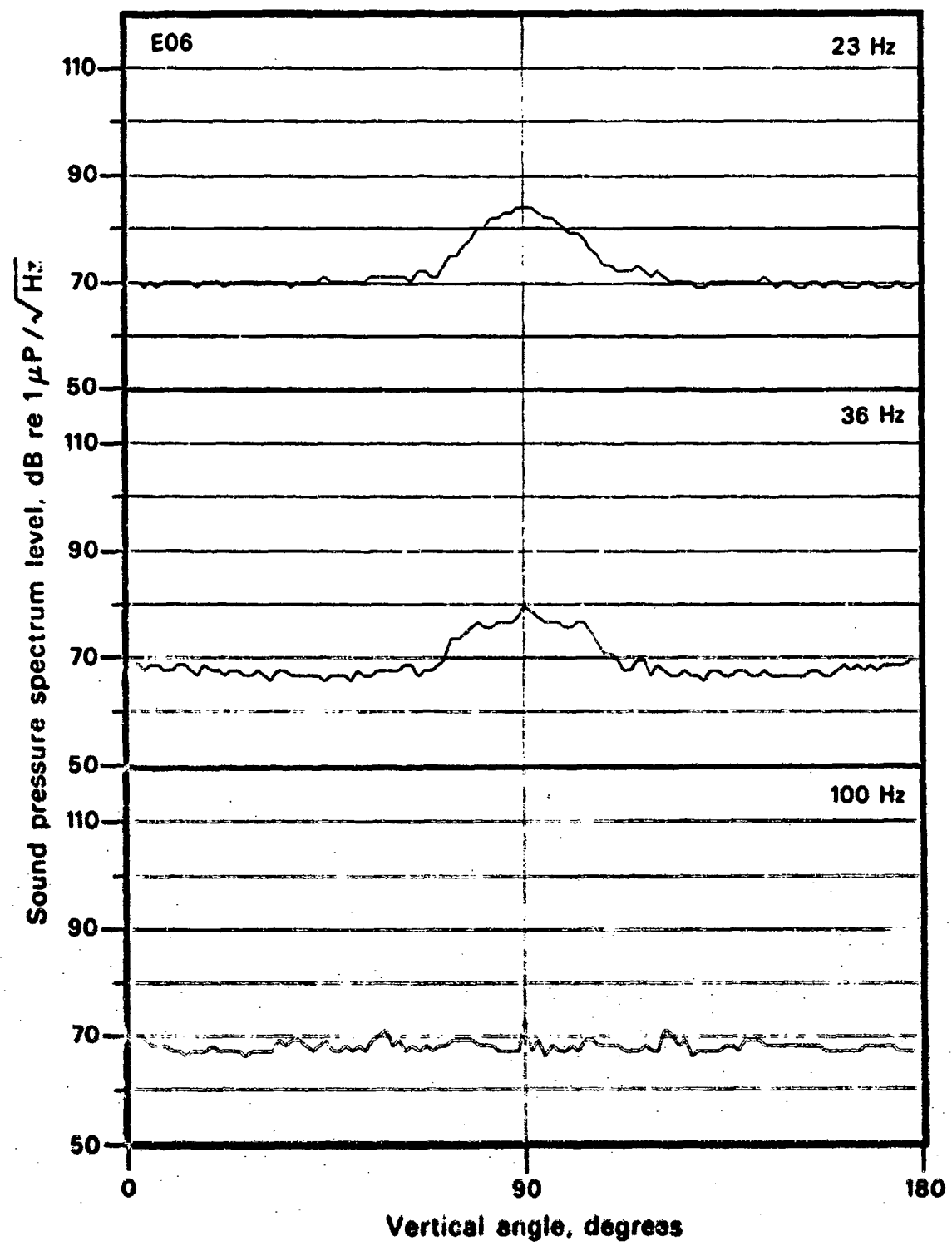


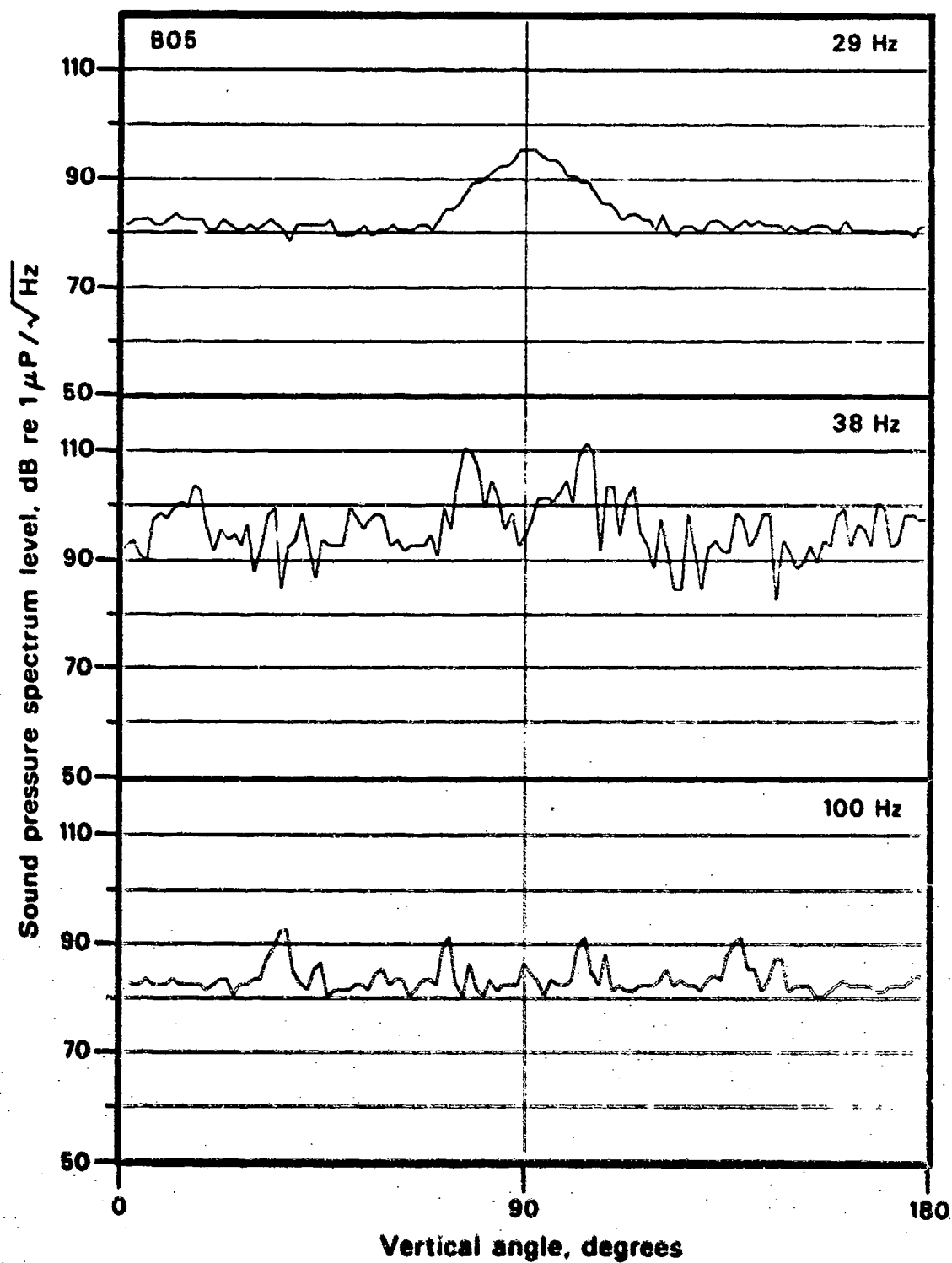


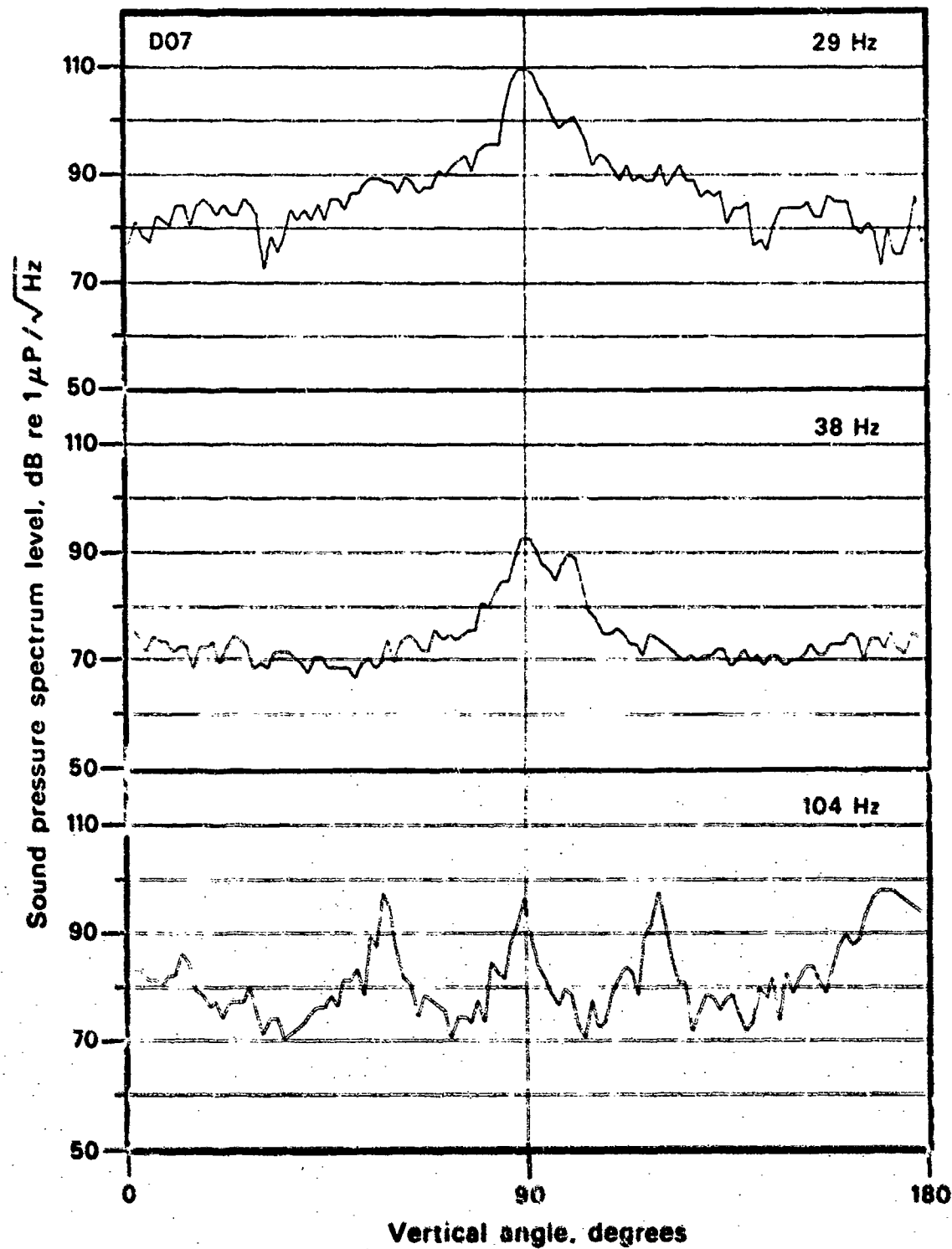


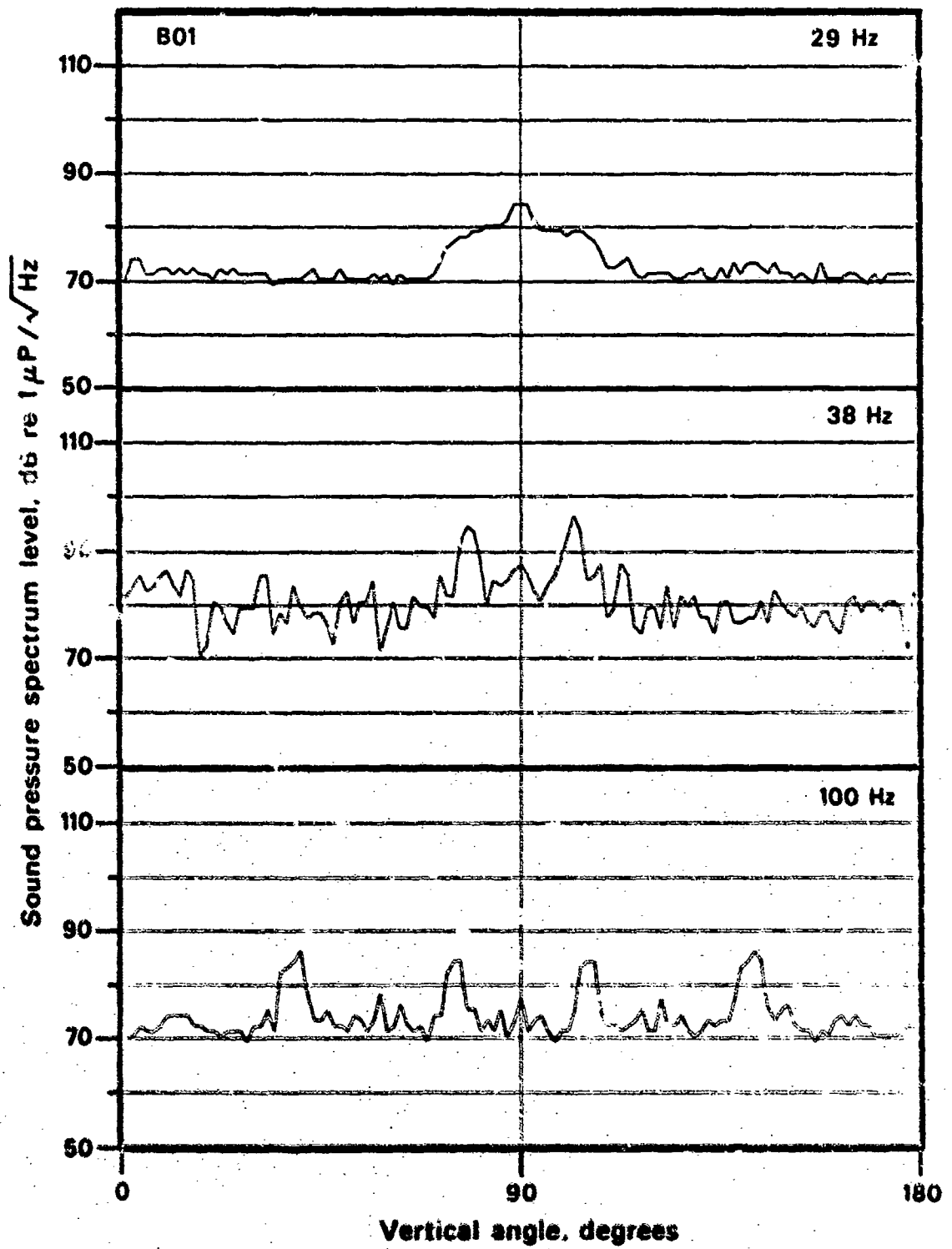


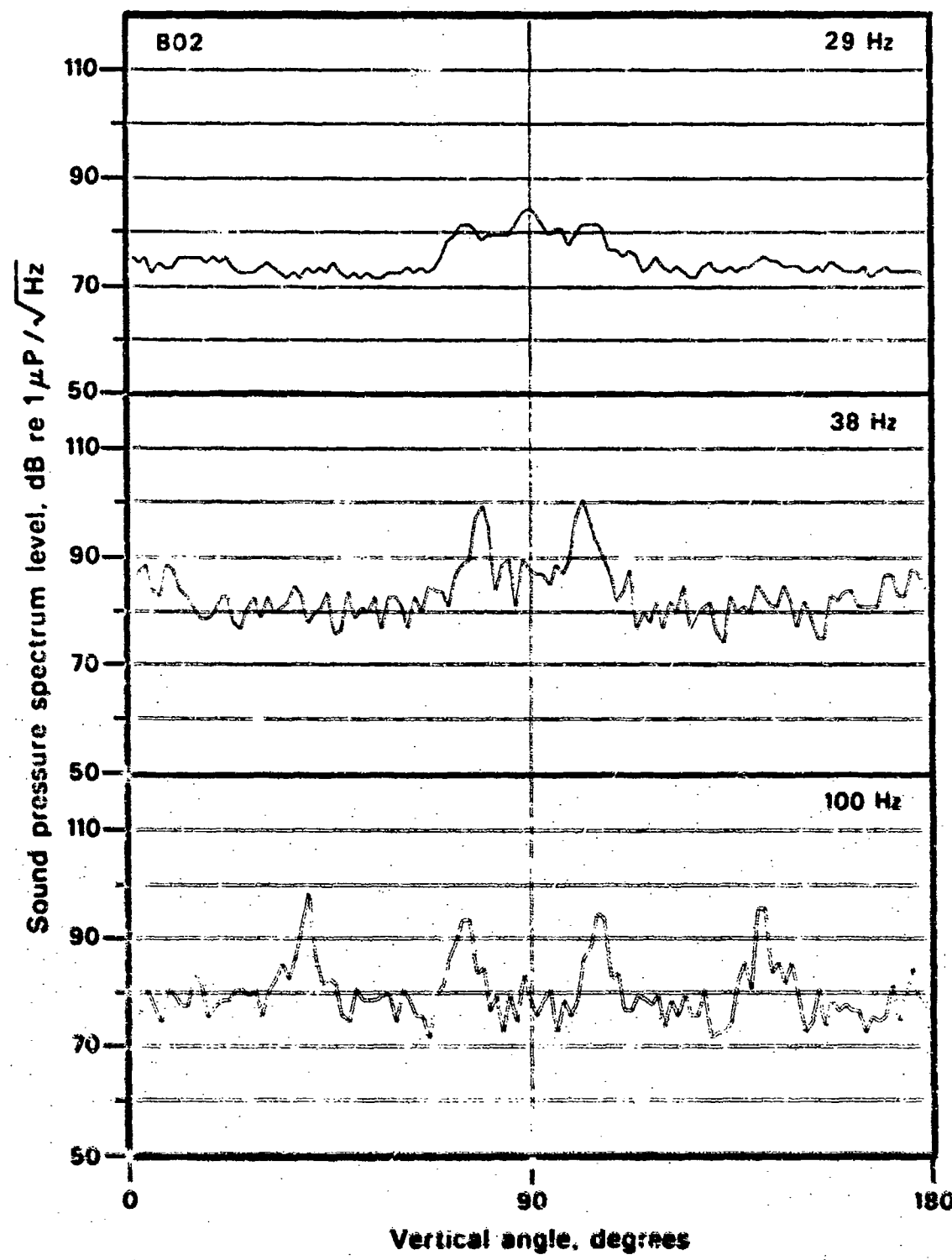


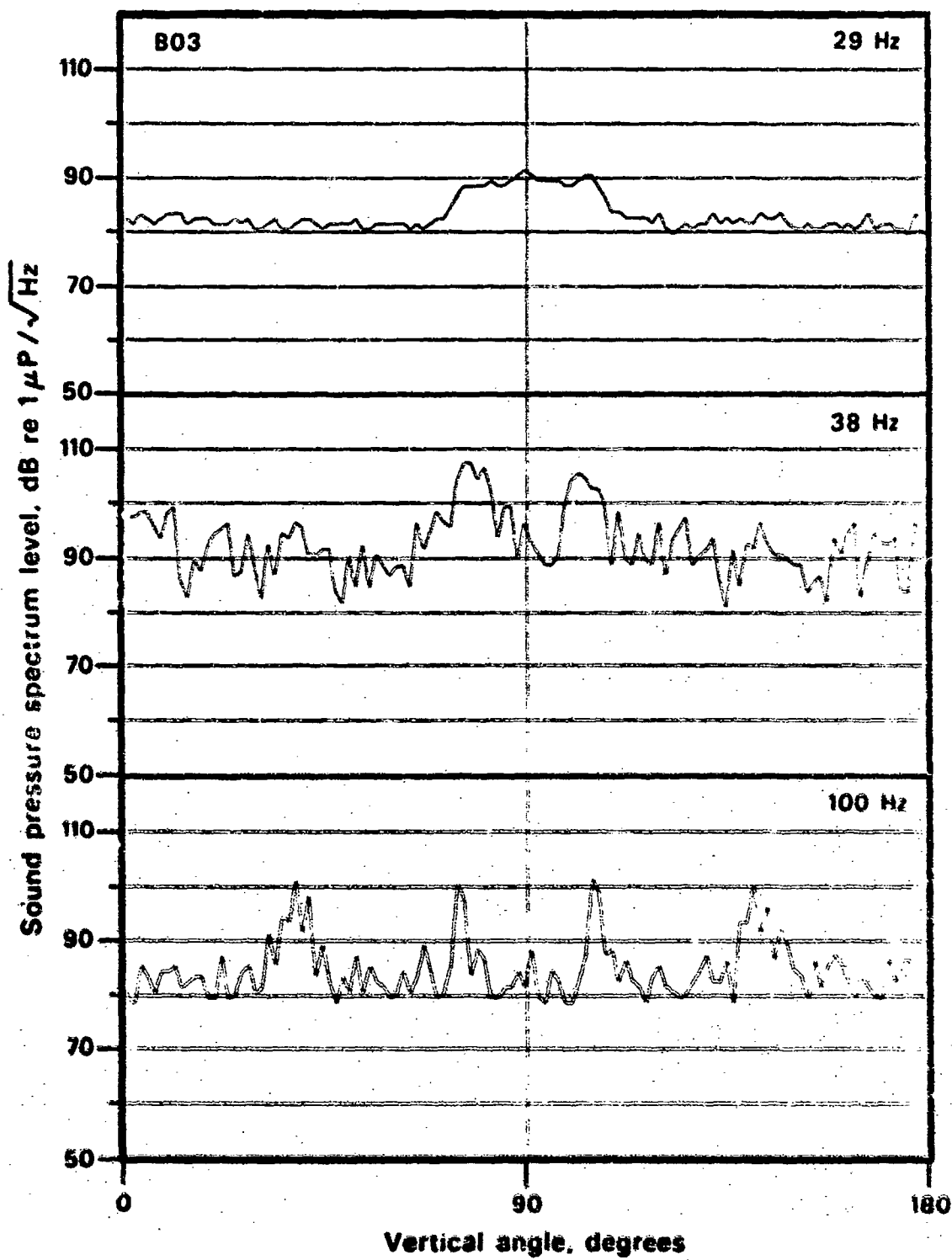


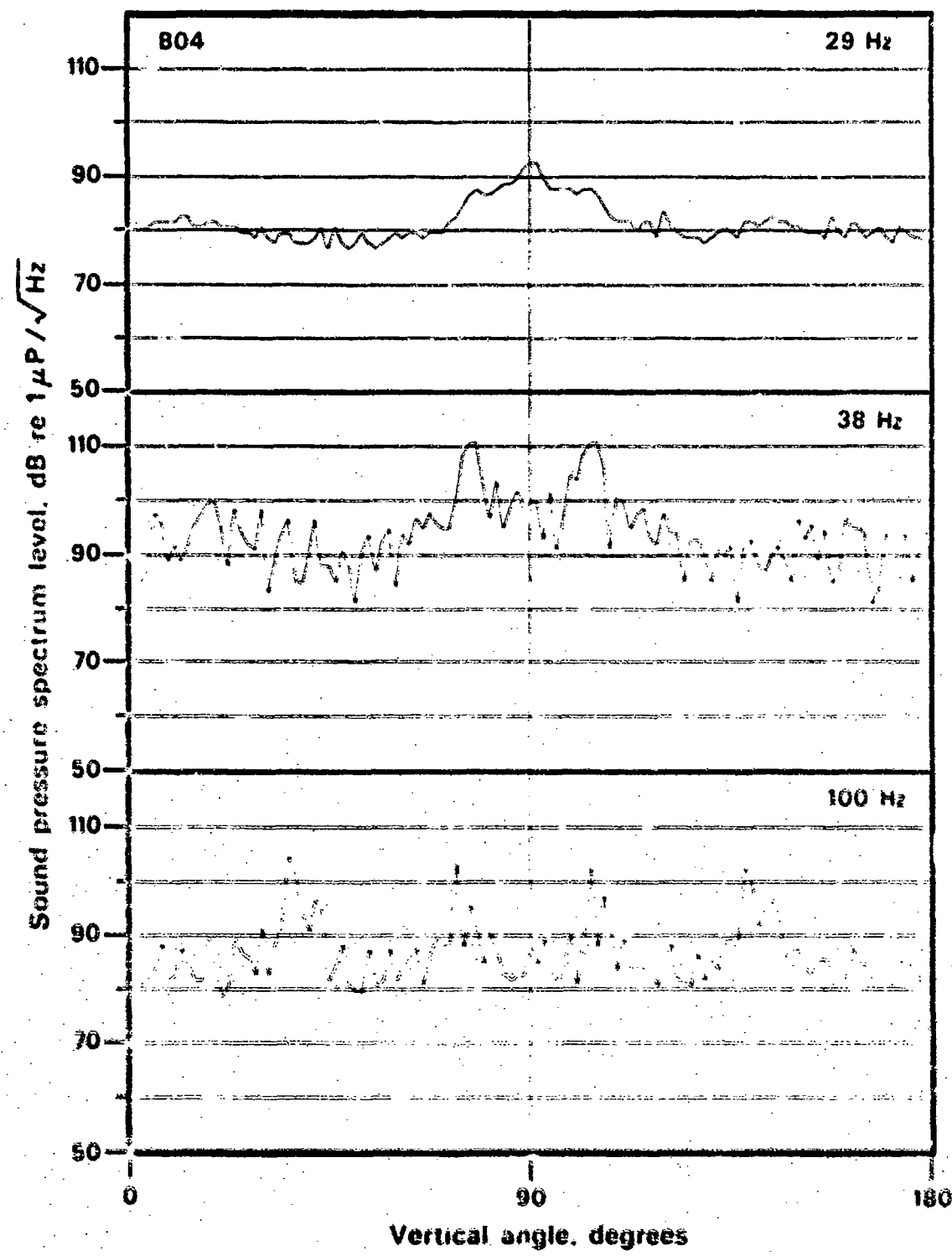


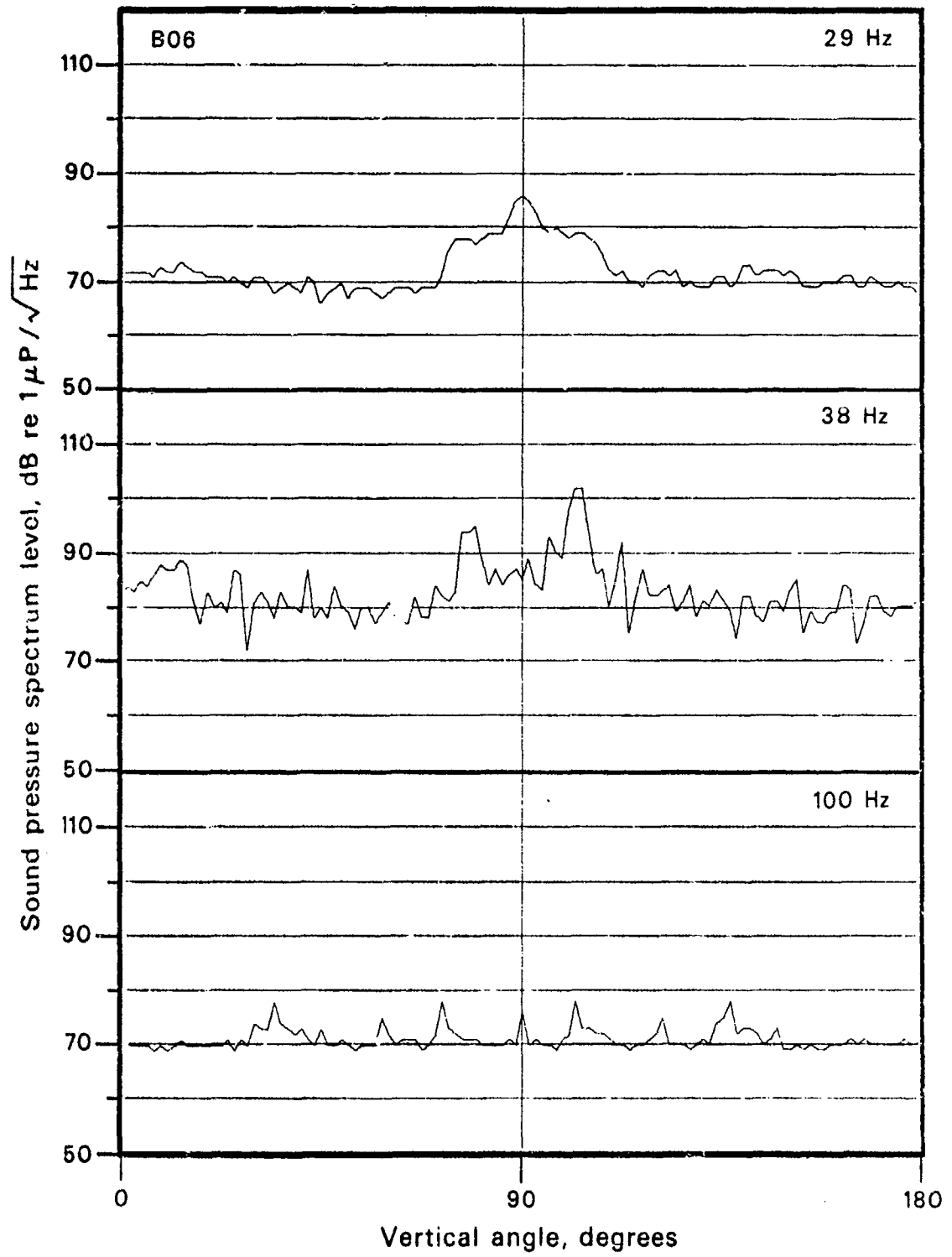


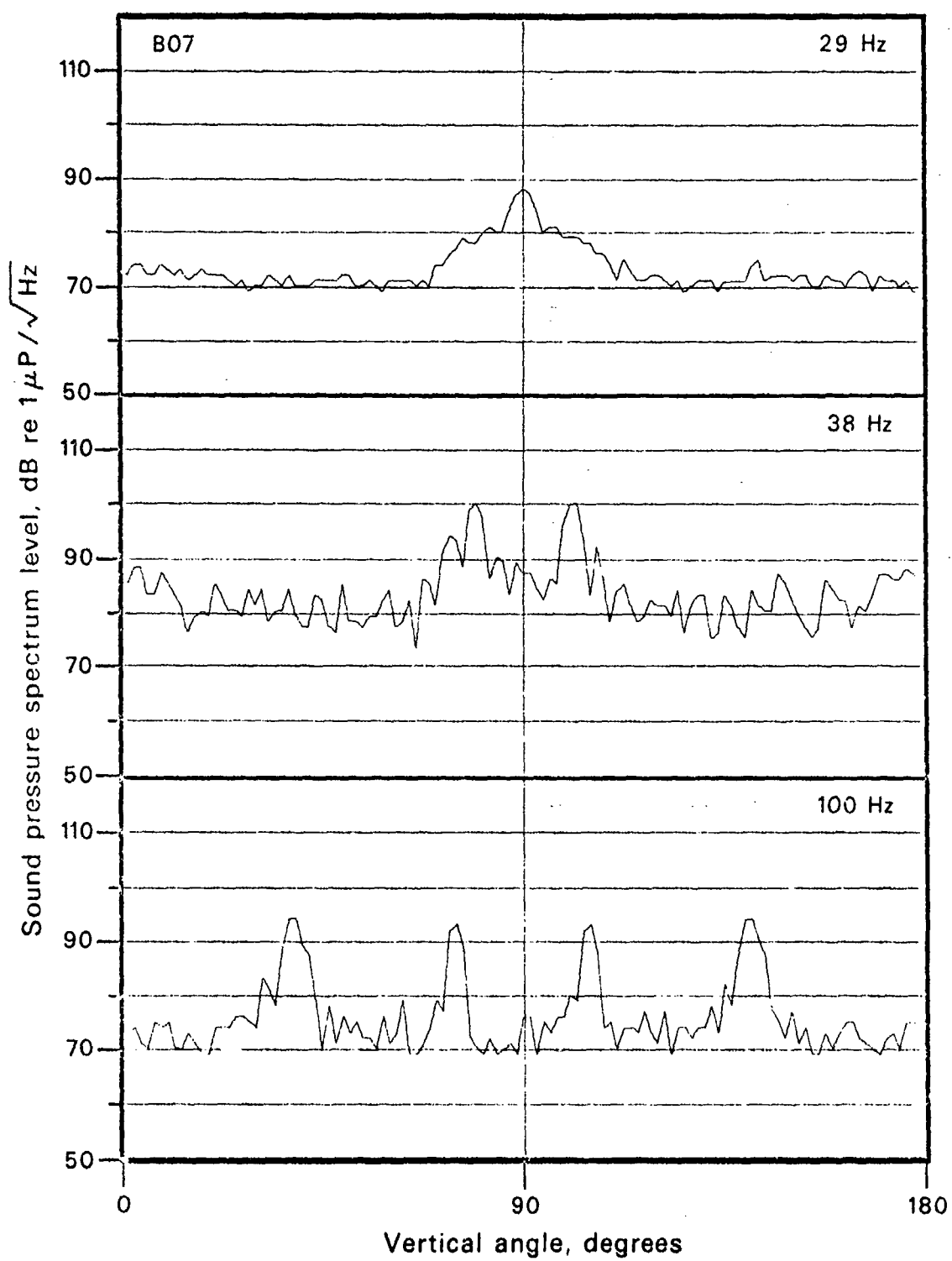


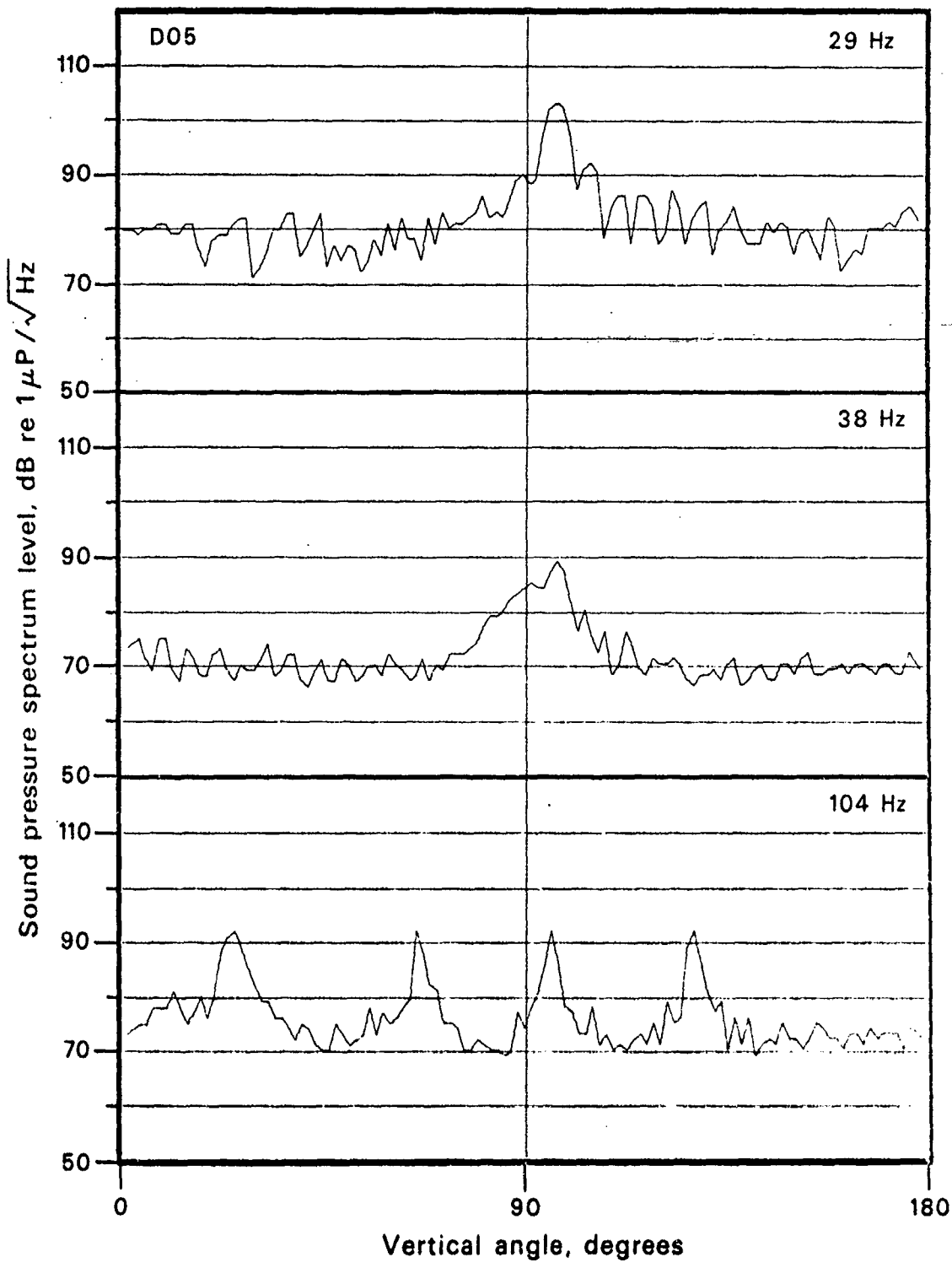


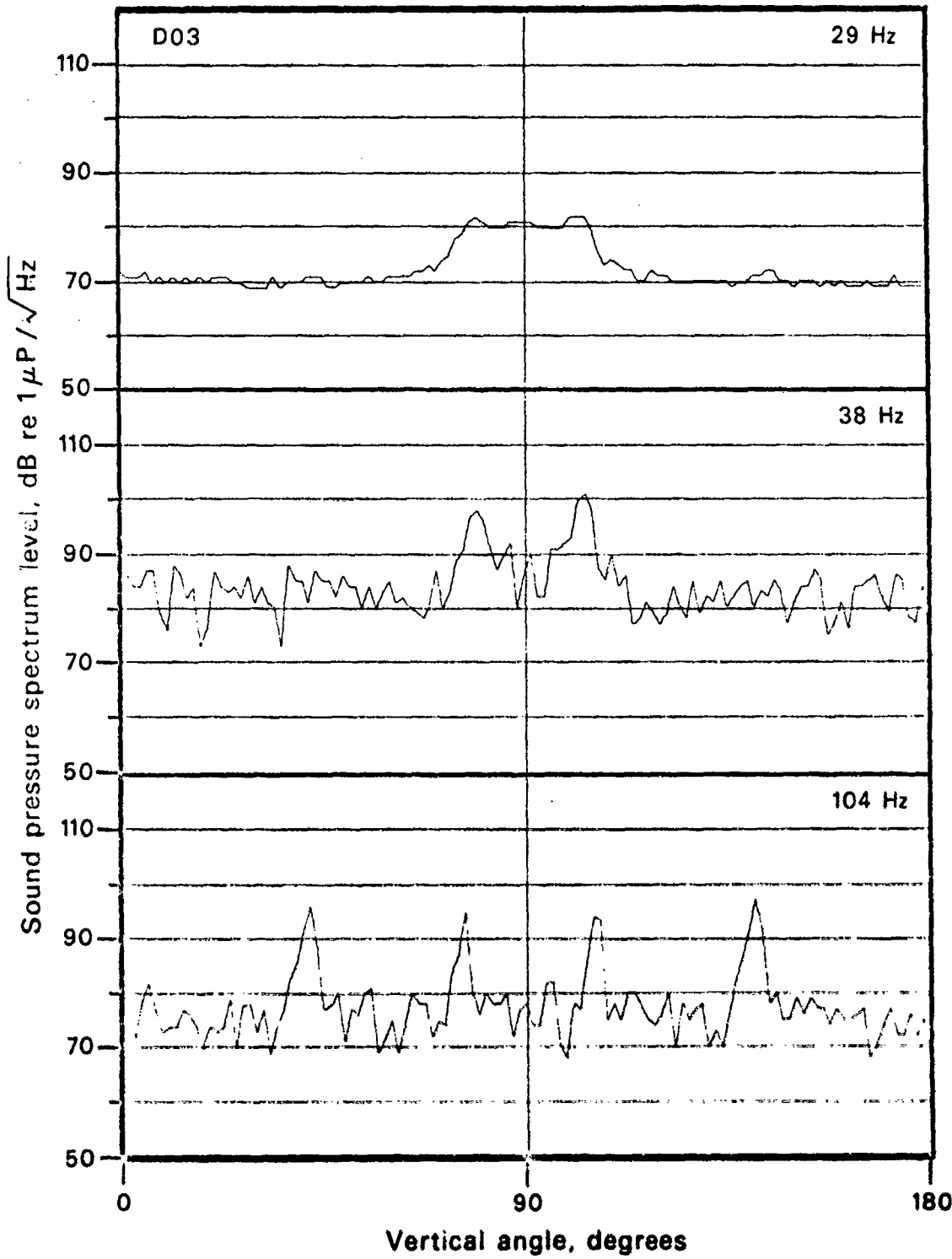


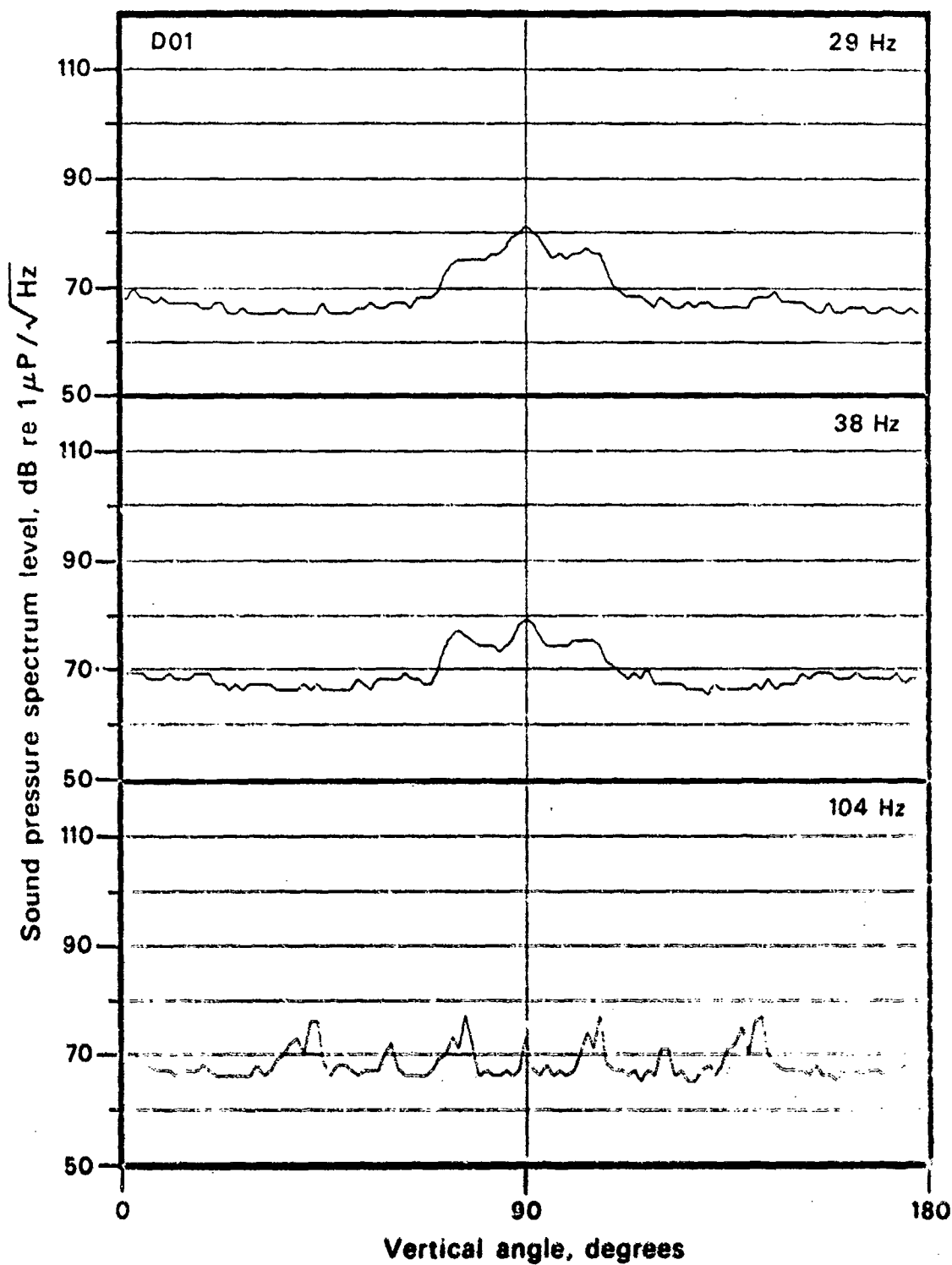


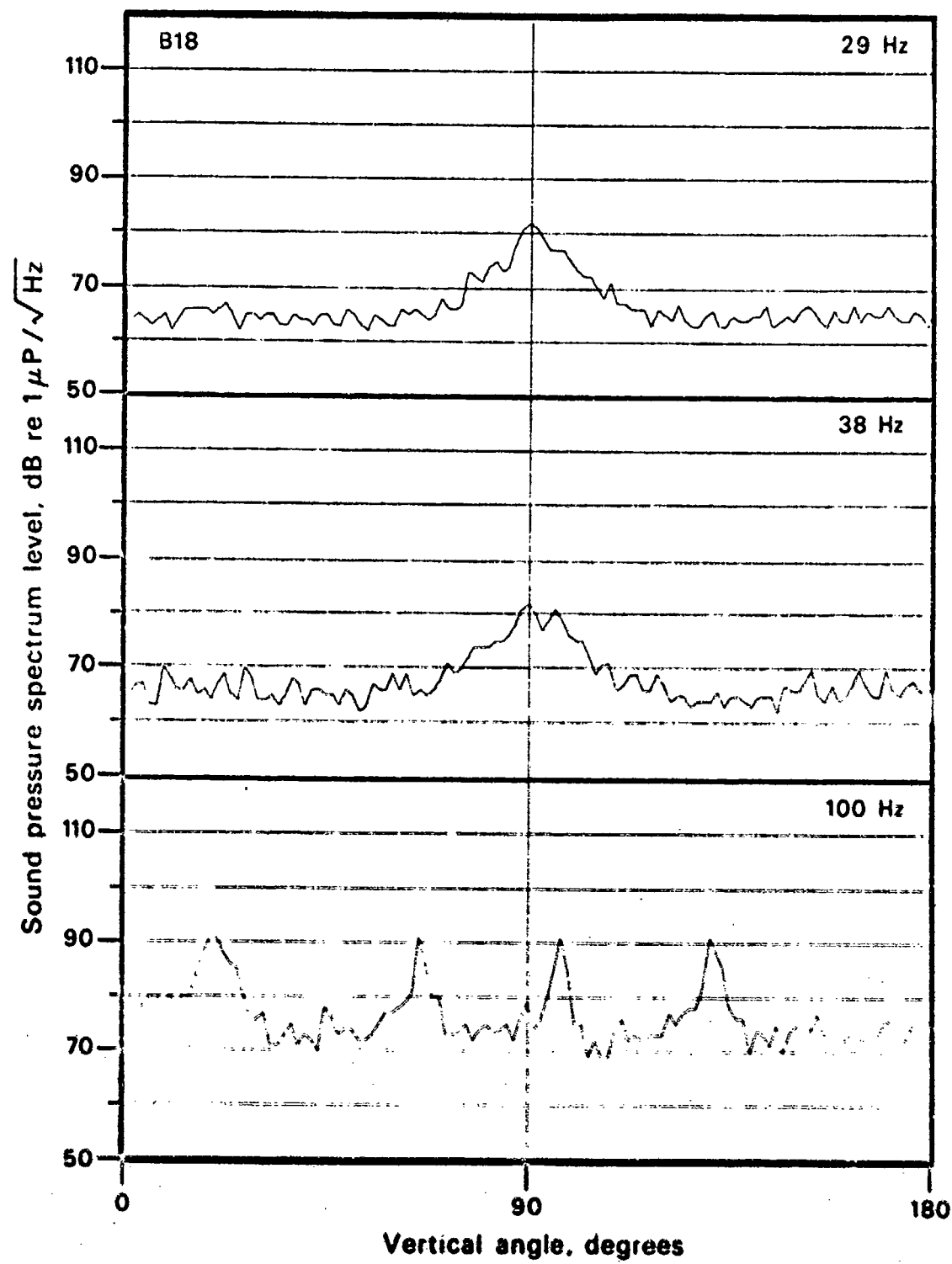


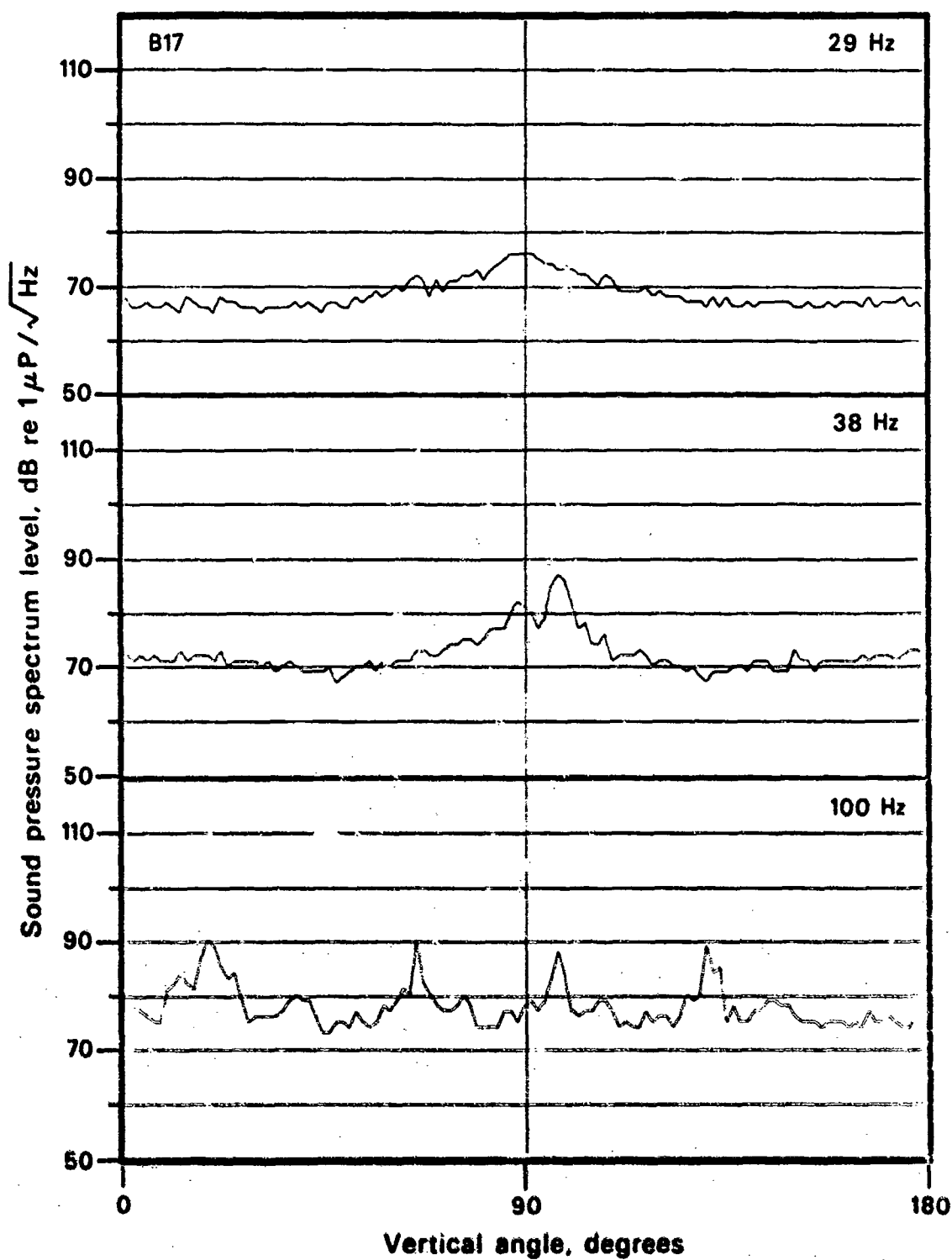


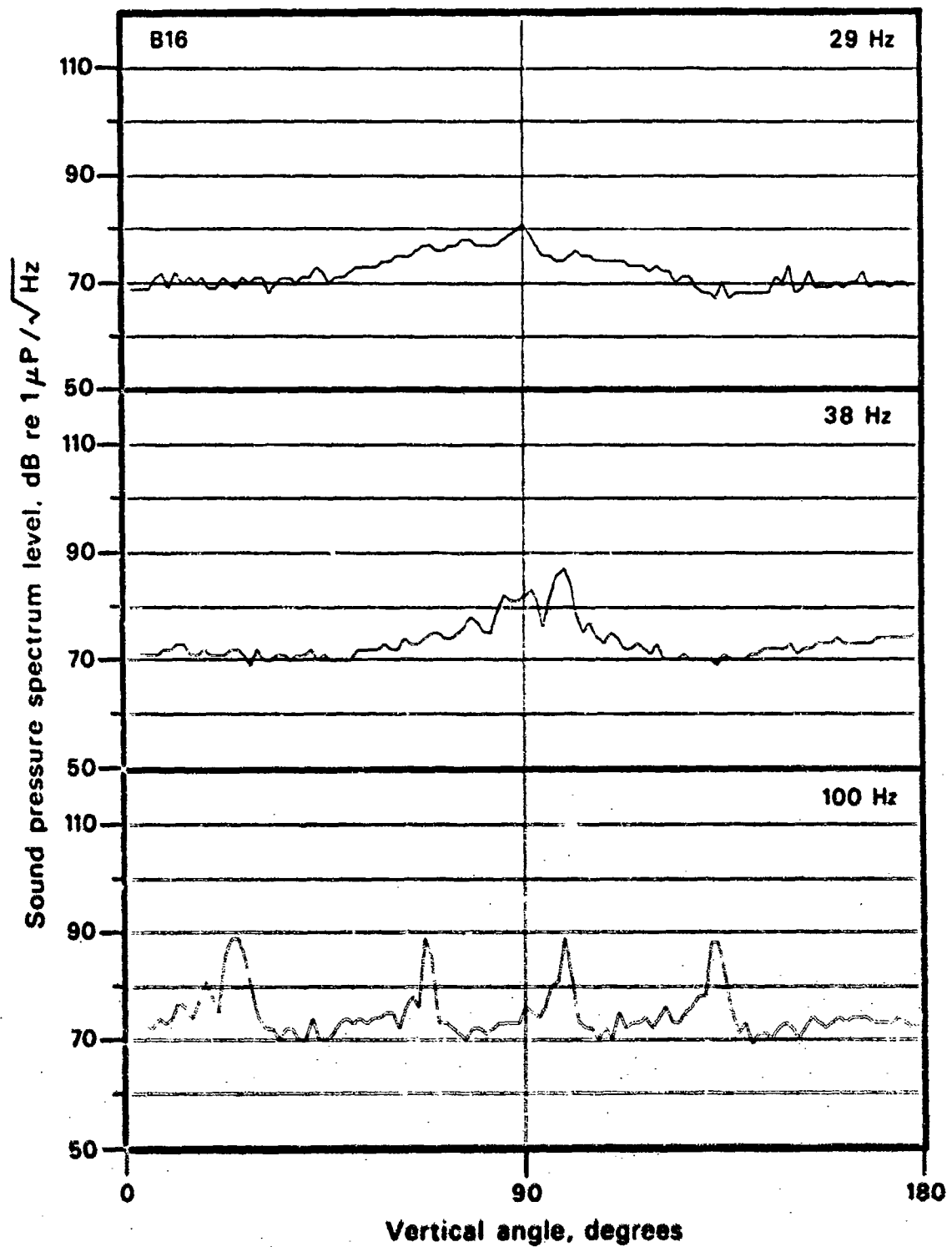


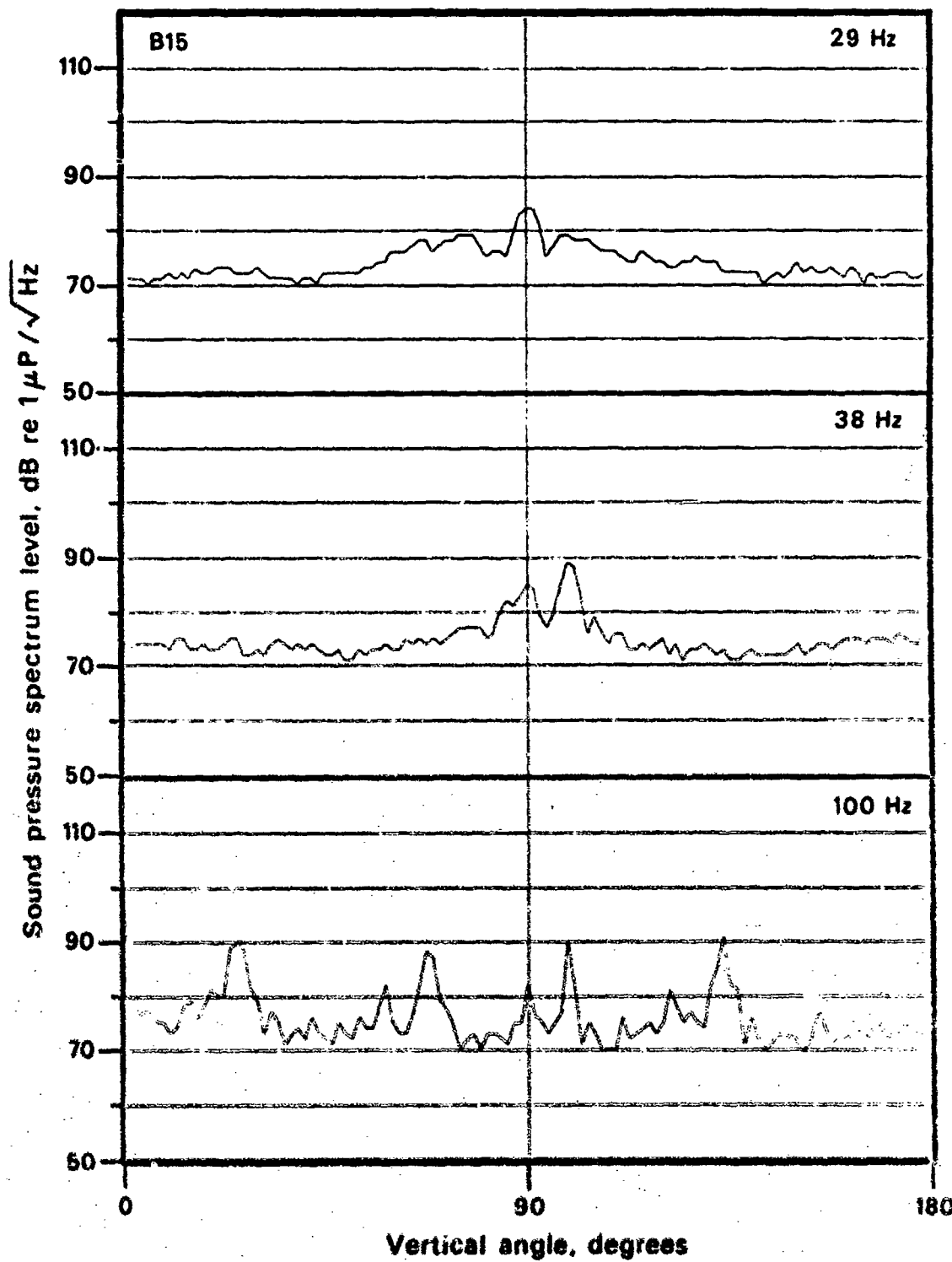


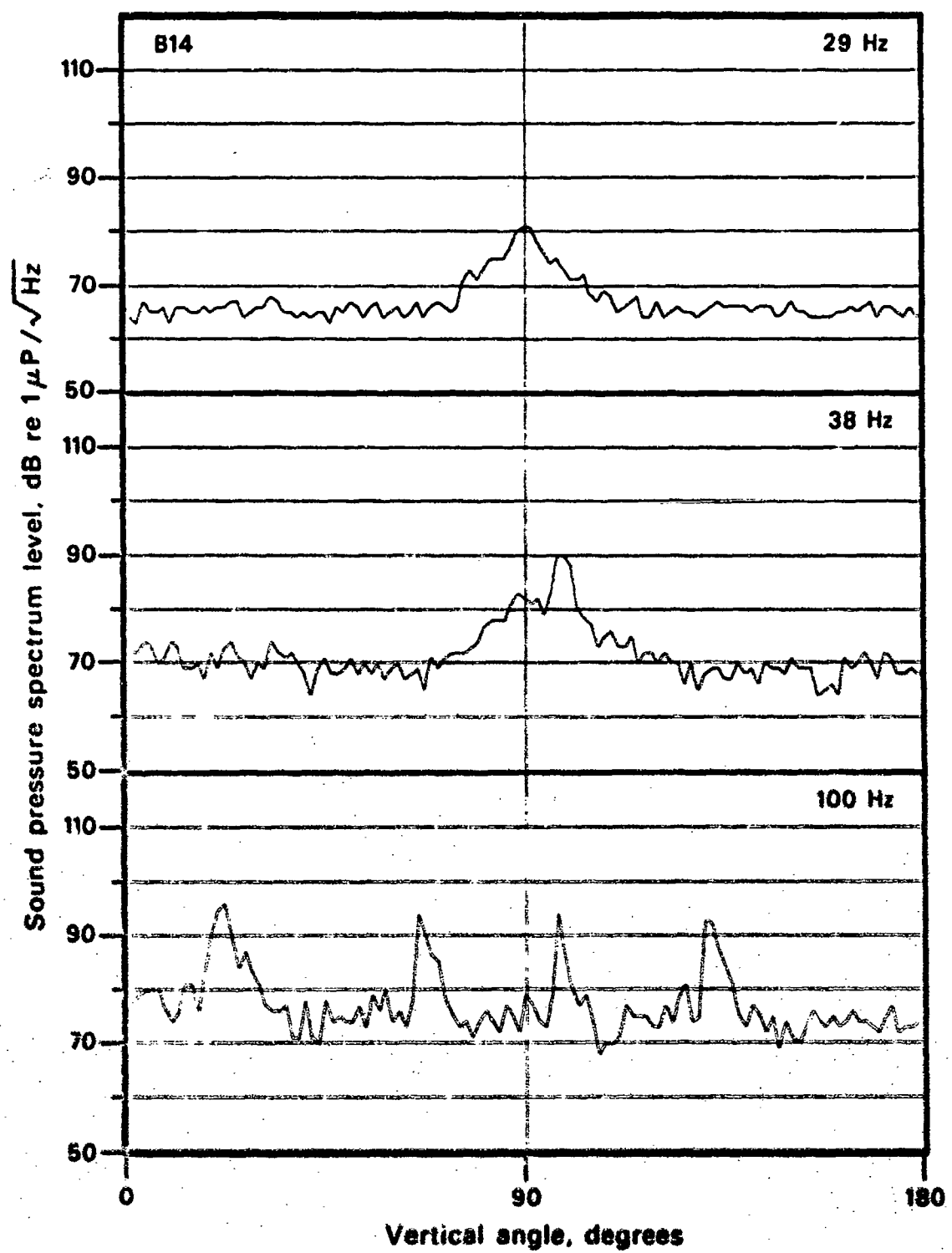


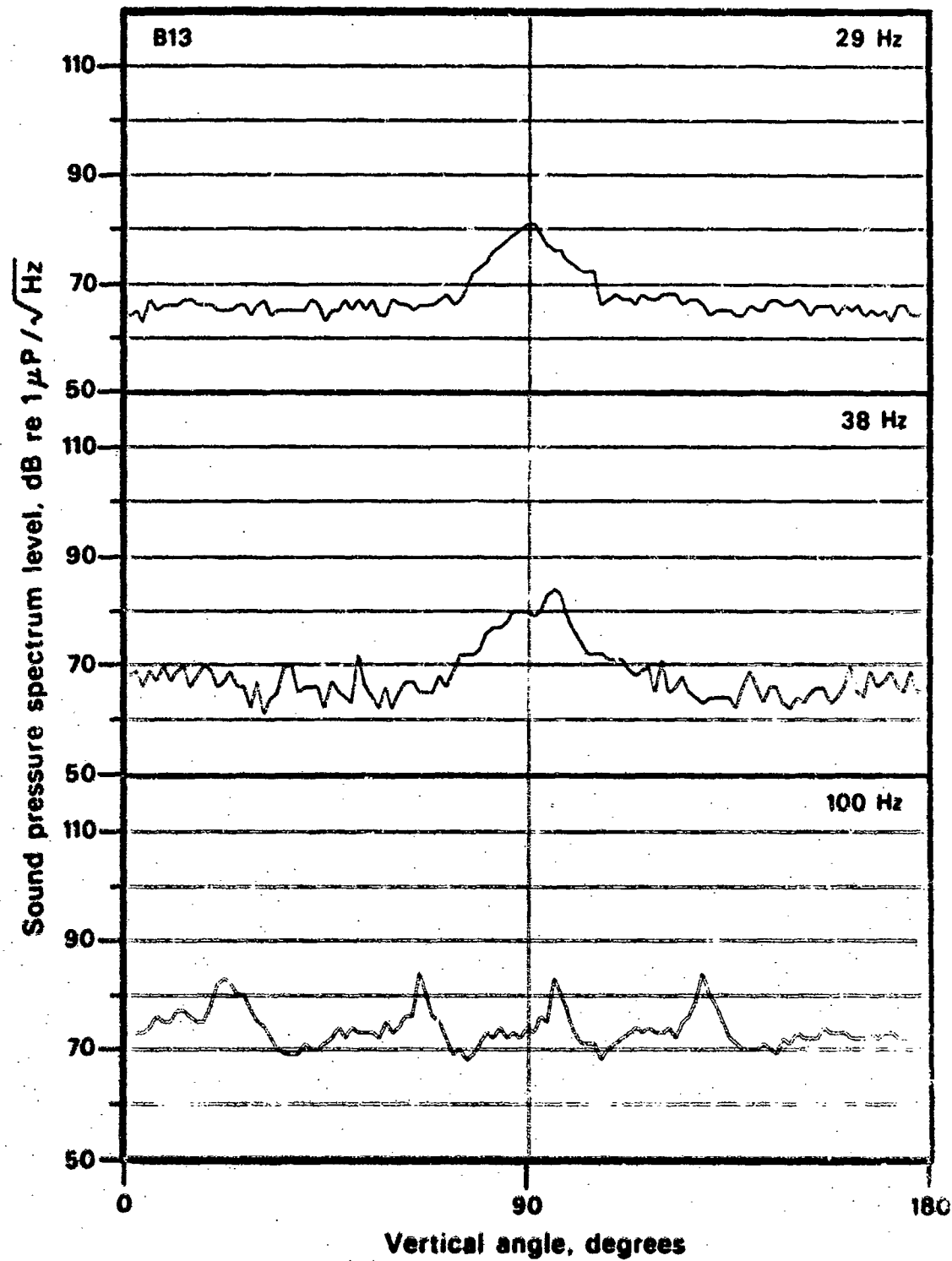


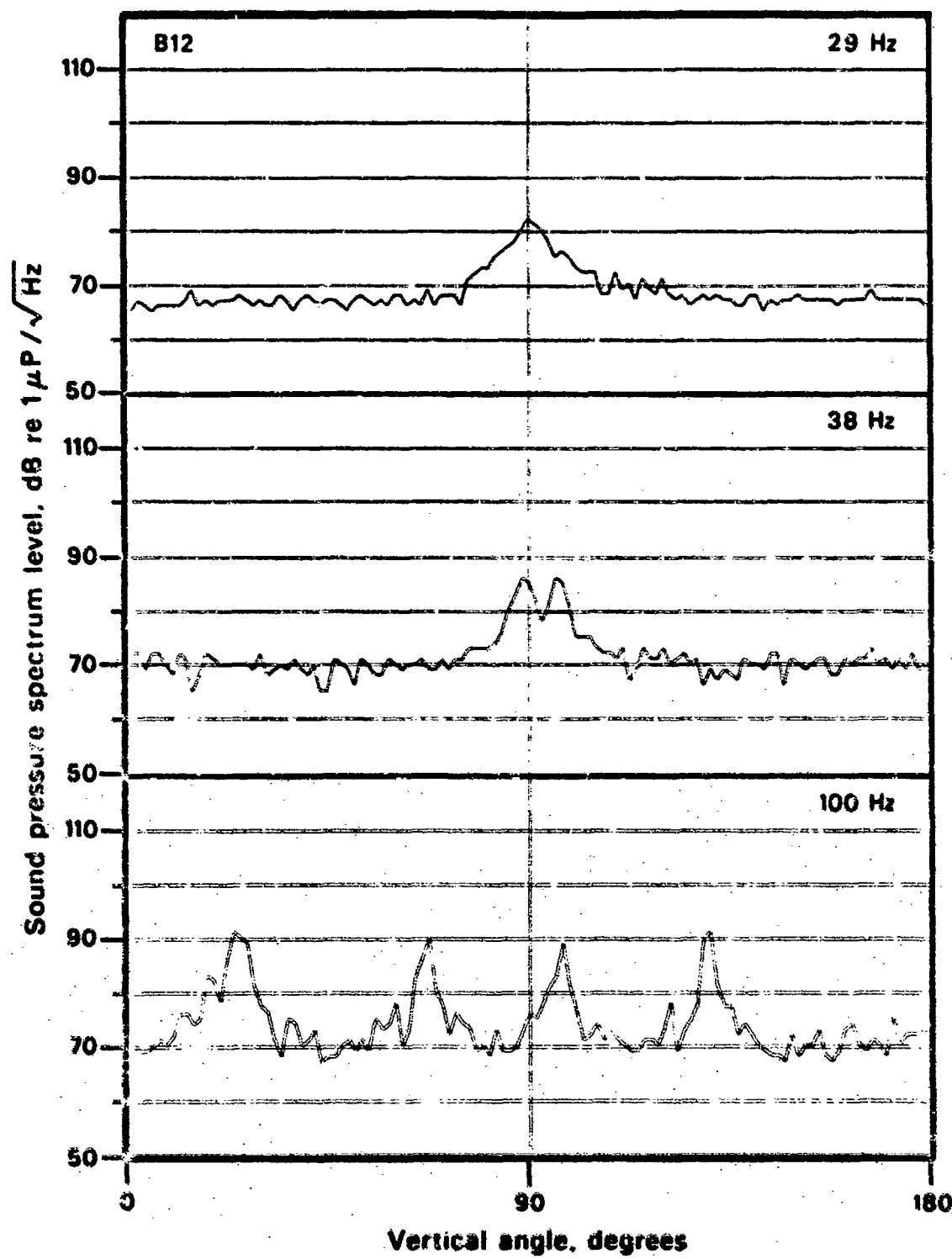


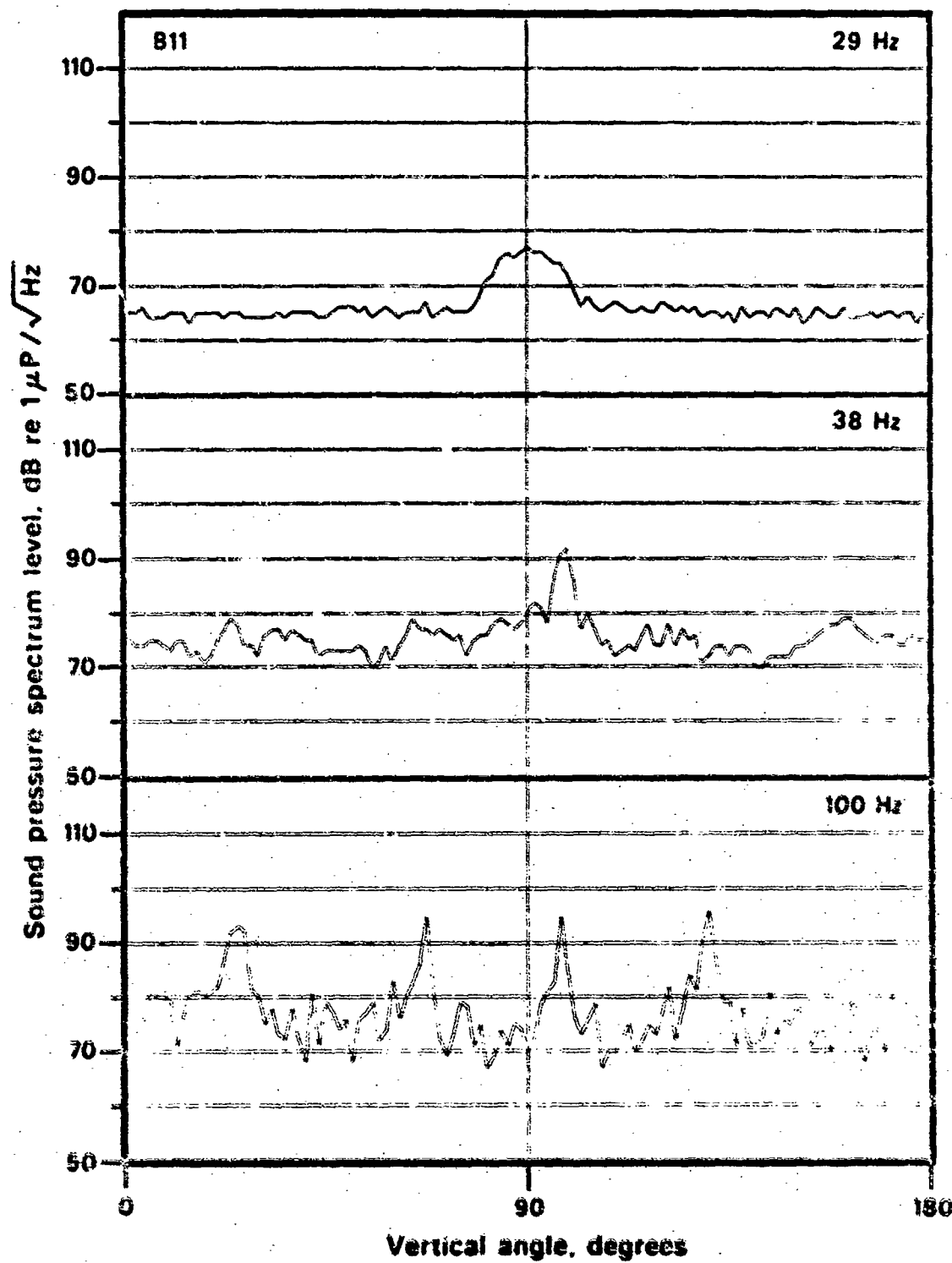


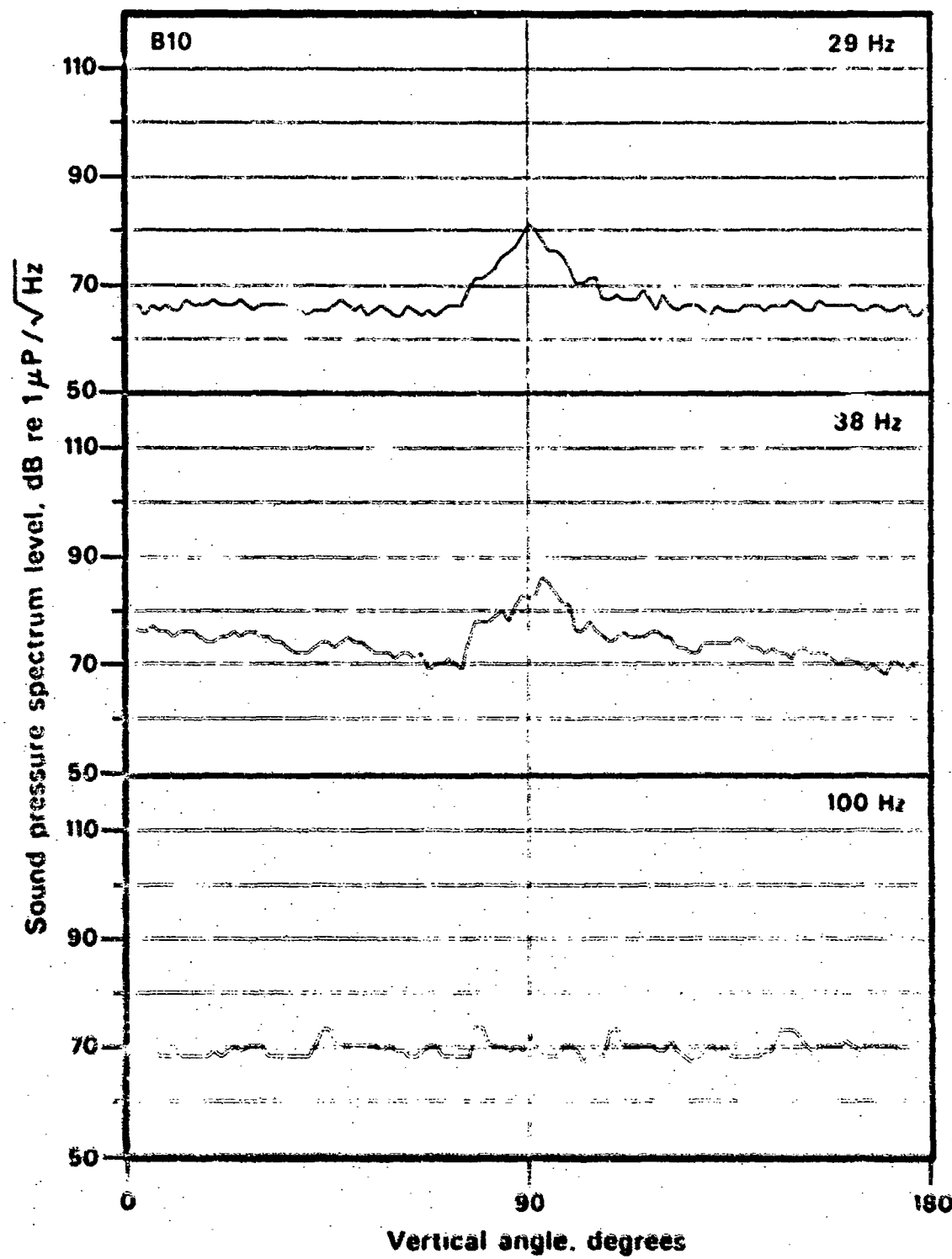


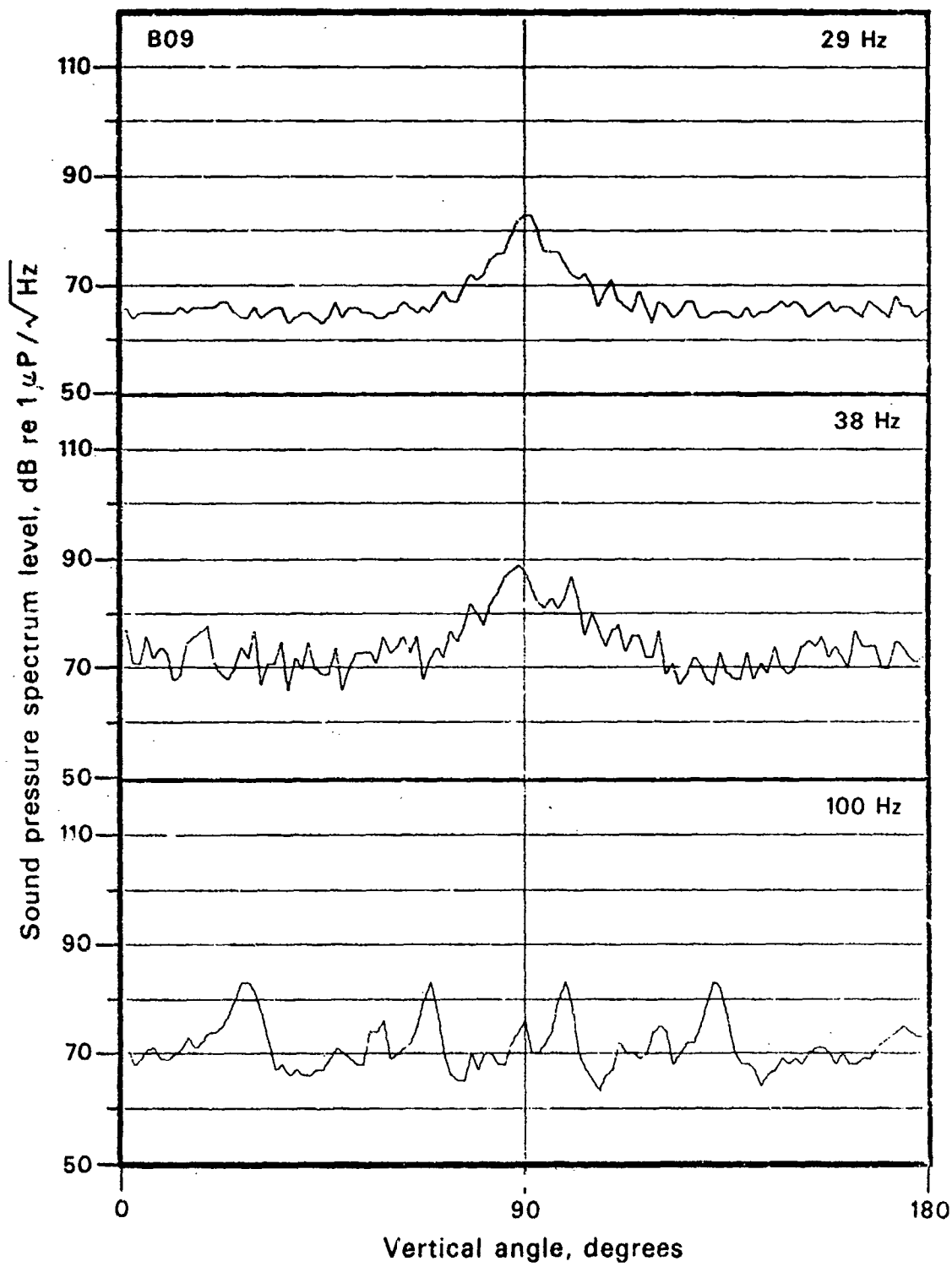


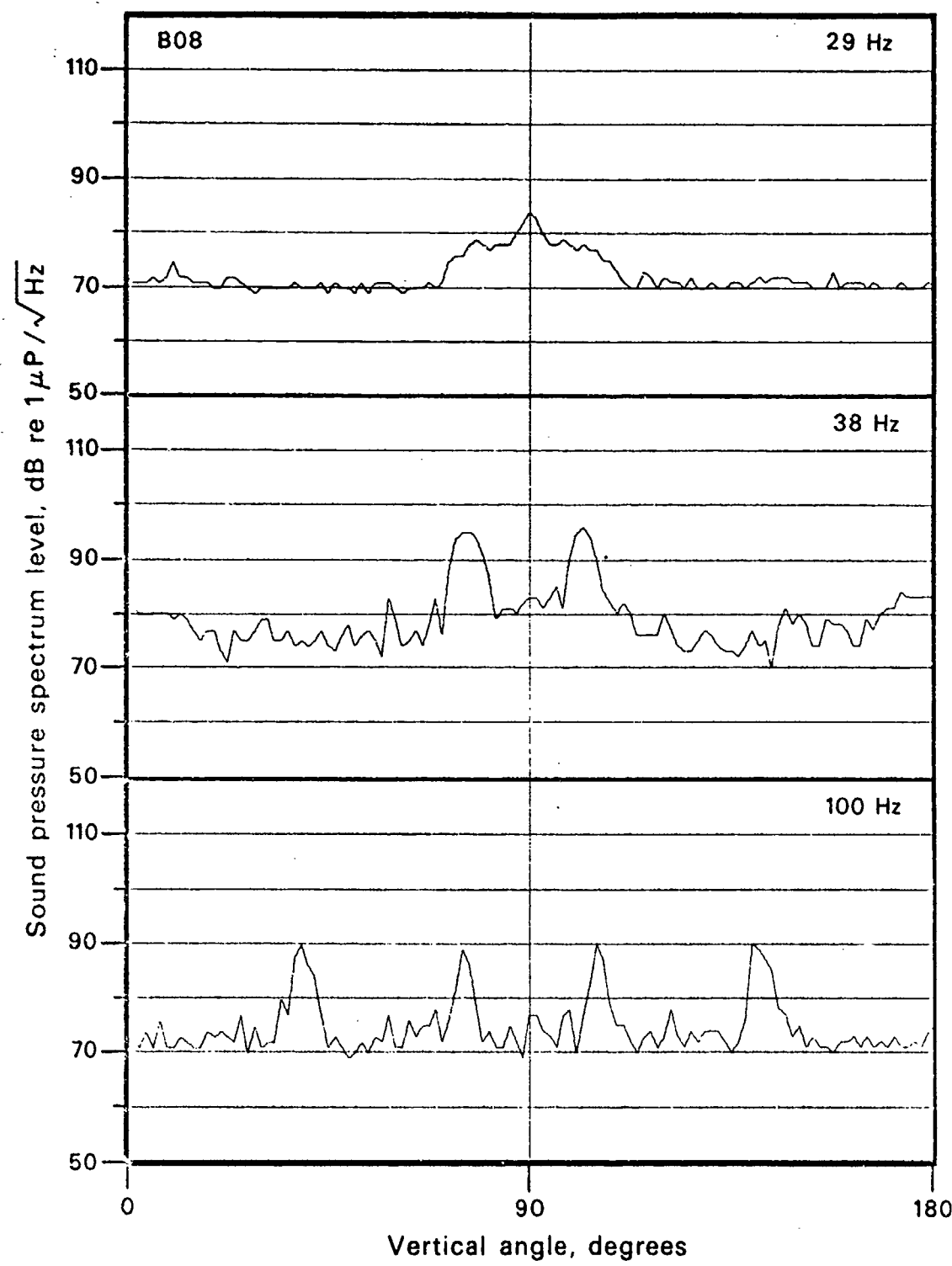














DEPARTMENT OF THE NAVY

OFFICE OF NAVAL RESEARCH
875 NORTH RANDOLPH STREET
SUITE 1425
ARLINGTON VA 22203-1995

IN REPLY REFER TO:

5510/1
Ser 321OA/011/06
31 Jan 06

MEMORANDUM FOR DISTRIBUTION LIST

Subj: DECLASSIFICATION OF LONG RANGE ACOUSTIC PROPAGATION PROJECT (LRAPP) DOCUMENTS

Ref: (a) SECNAVINST 5510.36

Encl: (1) List of DECLASSIFIED LRAPP Documents

1. In accordance with reference (a), a declassification review has been conducted on a number of classified LRAPP documents.
2. The LRAPP documents listed in enclosure (1) have been downgraded to UNCLASSIFIED and have been approved for public release. These documents should be remarked as follows:

Classification changed to UNCLASSIFIED by authority of the Chief of Naval Operations (N772) letter N772A/6U875630, 20 January 2006.

DISTRIBUTION STATEMENT A: Approved for Public Release; Distribution is unlimited.

3. Questions may be directed to the undersigned on (703) 696-4619, DSN 426-4619.

BRIAN LINK
By direction

Subj: DECLASSIFICATION OF LONG RANGE ACOUSTIC PROPAGATION PROJECT
(LRAPP) DOCUMENTS

DISTRIBUTION LIST:

NAVOCEANO (Code N121LC – Jaime Ratliff)
NRL Washington (Code 5596.3 – Mary Templeman)
PEO LMW Det San Diego (PMS 181)
DTIC-OCQ (Larry Downing)
ARL, U of Texas
Blue Sea Corporation (Dr. Roy Gaul)
ONR 32B (CAPT Paul Stewart)
ONR 321OA (Dr. Ellen Livingston)
APL, U of Washington
APL, Johns Hopkins University
ARL, Penn State University
MPL of Scripps Institution of Oceanography
WHOI
NAVSEA
NAVAIR
NUWC
SAIC

Declassified LRAPP Documents

Report Number	Personal Author	Title	Publication Source (Originator)	Pub. Date	Current Availability	Class.
Unavailable	Beam, J. P., et al.	LONG-RANGE ACOUSTIC PROPAGATION LOSS MEASUREMENTS OF PROJECT TRANSLANT I IN THE ATLANTIC OCEAN EAST OF BERMUDA	Naval Underwater Systems Center	740612	ADC001521	U
Unavailable	Cornyn, J. J., et al.	AMBIENT-NOISE PREDICTION. VOLUME 2. MODEL EVALUATION WITH JOMEDEX DATA	Naval Research Laboratory	740701	AD0530983	U
Unavailable	Unavailable	COHERENCE OF HARMONICALLY RELATED CW SIGNALS	Naval Underwater Systems Center	740722	ADB181912	U
Unavailable	Banchero, L. A., et al.	JOMEDEX SOUND VELOCITY ANALYSIS AND ENVIRONMENTAL DATA SUMMARY	Naval Oceanographic Office	740801	ADC00419	U
3810	Unavailable	CONSTRUCTION AND CALIBRATION OF USRD TYPE F58 VIBROSEIS MONITORING HYDROPHONES SERIALS 1 THROUGH 7	Naval Research Laboratory	741002	ND	U
ARL-TM-73-11; ARL-TM-73-12	Ellis, G. E., et al.	ARL PRELIMINARY DATA ANALYSIS FROM ACODAC SYSTEM; ANALYSIS OF THE BLAKE TEST ACODAC DATA	University of Texas, Applied Research Laboratories	741015	ADA001738; ND	U
Unavailable	Mitchell, S. K., et al.	QUALITY CONTROL ANALYSIS OF SUS PROCESSING FROM ACODAC DATA	University of Texas, Applied Research Laboratories	741015	ADB000283	U
Unavailable	Unavailable	MEDEX PROCESSING SYSTEM. VOLUME II. SOFTWARE	Bunker-Ramo Corp. Electronic Systems Division	741021	ADB000363	U
Unavailable	Spofford, C. W.	FACT MODEL. VOLUME I	Maury Center for Ocean Science	741101	ADA078581	U
Unavailable	Bucca, P. J., et al.	SOUND VELOCITY STRUCTURE OF THE LABRADOR SEA, IRMINGER SEA, AND BAFFIN BAY DURING THE NORULANT-72 EXERCISE	Naval Oceanographic Office	741101	ADC000461	U
Unavailable	Anderson, V. C.	VERTICAL DIRECTIONALITY OF NOISE AND SIGNAL TRANSMISSIONS DURING OPERATION CHURCH ANCHOR	Scripps Institution of Oceanography Marine Physical Laboratory	741115	ADA011110	U
Unavailable	Baker, C. L., et al.	FACT MODEL. VOLUME II	Office of Naval Research	741201	ADA078539	U
ARL-TR-74-53	Anderson, A. L.	CHURCH ANCHOR EXPLOSIVE SOURCE (SUS) PROPAGATION MEASUREMENTS (U)	University of Texas, Applied Research Laboratories	741201	ADC002497; ND	U
MCR106	Cherkis, N. Z., et al.	THE NEAT 2 EXPERIMENT VOL 1 (U)	Maury Center for Ocean Science	741201	NS; ND	U
MCR107	Cherkis, N. Z., et al.	THE NEAT 2 EXPERIMENT VOL 2 - APPENDICES (U)	Maury Center for Ocean Science	741201	NS; ND	U
Unavailable	Mahler, J., et al.	INTERIM SHIPPING DISTRIBUTION	Tetra, Tech, BB&N, & PSI	741217	ND	U
75-9M7-VERRAY-R1	Jones, C. H.	LRAPP VERTICAL ARRAY- PHASE IV	Westinghouse Electric Corp.	750113	ADA008427; ND	U
AESD-TN-75-01	Spofford, C. W.	ACOUSTIC AREA ASSESSMENT	Office of Naval Research	750201	ADA090109; ND	U